JOC The Journal of Organic Chemistry

Perspective

Two-Phase Total Synthesis of Taxanes: Tactics and Strategies

Yuzuru Kanda, Yoshihiro Ishihara, Nathan Wilde, and Phil S. Baran

J. Org. Chem., **Just Accepted Manuscript** • DOI: 10.1021/acs.joc.0c01287 • Publication Date (Web): 14 Jul 2020

Two-Phase Total Synthesis of Taxanes: Tactics and Strategies

Yuzuru Kanda, Yoshihiro Ishihara,[†] Nathan C. Wilde,[†] Phil S. Baran[*]

Department of Chemistry, Scripps Research, 10550 North Torrey Pines Road, La Jolla, CA 92037, United States.
[*]E-mail: pbaran@scripps.edu

ABSTRACT: This perspective goes into the fine details of our laboratory's quest to answer a longstanding fundamental question: Could any new approach to terpene synthesis, perhaps one patterned on biosynthesis, enable a divergent synthetic approach to the taxane family of natural products? We targeted Taxol®, the flagship taxane, as the upper limit of chemical complexity and employed two-phase terpene synthesis logic as the guiding strategy. The first synthesis target was taxadiene, the lowest oxidized member of the taxane family, followed by three site-selective allylic oxidations at C5, C10, and C13, which led to the two-phase synthesis of taxuyunnanine D. Successful C9 oxidation enabled access to a wider range of taxanes, which was demonstrated by the two-phase synthesis of decinnamoyltaxinine E and taxabaccatin III. The final two sp^3 C–H oxidations at C1 and C7 were attained by dioxirane-mediated C–H oxidation and an oxidation relay based on judicious substrate design, culminating in a two-phase synthesis of Taxol®. The purpose of this perspective is to articulate strategies and tactics developed for the two-phase synthesis of taxanes, whose lessons can be potentially extrapolated to medicinal chemistry endeavors in the taxane family, as well as to the synthesis of other terpene families.

CONTENTS

1. Introduction

1.1 Background of Taxol®

Taxol® (**1.1**; Figure 1) is a natural product of great significance:[1,2] its potent anticancer activity led to worldwide academic and industrial research, resulting in its use as a life-saving medicine since 1992.[3,4] It is still prescribed today in generic form as paclitaxel, and in alternative formulations such as Abraxane® (albumin-bound).[5] There is also a structural derivative called Taxotere®, which, together with Taxol® (**1.1**), are on the World Health Organization's List of Essential Medicines.[6,7]

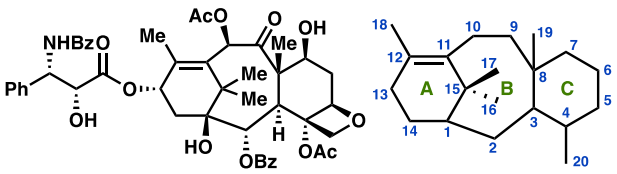

Taxol® (**1.1**, paclitaxel)

Figure 1. The structure of Taxol® (**1.1**) and its skeletal numbering system.

At the outset, procuring a large amount of Taxol® (**1.1**) relied on an environmentally destructive isolation process from the bark of the Pacific yew tree.[2] A semisynthetic route alleviated the environmental burden, as the building blocks were then isolated from a renewable resource (twigs and needles from the European yew tree).[8–10] More recently, a synthetic-biology-based route using plant cell fermentation (PCF) technology has allowed the direct preparation of **1.1** on metric ton scale.[11,12]

Taxol® (**1.1**) and related taxanes comprise a large family of more than 450 diterpene natural products.[13] Structurally, **1.1** is a polycyclic diterpene possessing a conformationally flexible medium-sized ring adorned with a multitude of similarly reactive secondary alcohols. The medicinal importance of Taxol® (**1.1**), coupled to the densely assembled functional groups and its unique 6-8-6 tricyclic carbon skeleton, has been of tremendous interest to the synthetic chemistry community.[14,15] In the early 1990s, at least 30 teams[16] competed in order to achieve the first synthesis of **1.1**. Even after the first synthesis, numerous groups investigated efficient synthetic routes to this molecule, which is reflected in their convergent retrosynthesis.[17–29] Although the supply problem is now solved thanks to PCF, all of these teams presented elegant synthetic routes, enriching the field of organic chemistry and educating >100 chemists in the art of synthesis. Even in recent years, research groups around the globe have been working on the synthesis of the taxane family, each of them testing new reaction methodologies,[30] technologies[26] or retrosynthetic logic.[31] What is common to the existing syntheses of Taxol® (**1.1**) is that actual taxane cores (compounds containing the full, non-rearranged, 20-carbon skeleton) are not accessed until very late in the synthetic sequence. This was done, presumably, to improve synthetic convergency. For molecules of this size and complexity, such a strategy is sensible from the perspective of conventional retrosynthetic analysis.[32]

1.2 Two-Phase Synthesis

Nature's terpene biosynthetic machinery is superior in producing maximum analog diversity from a common scaffold due to its encoded evolutionary logic. Thus, a synthesis campaign was initiated in 2007 to pattern the logic of two-phase biosynthesis onto a chemical synthesis of highly oxidized terpenes (e.g., eudesmantetraol; Figure 2 left)[33,34] in order to test the question of whether such a biomimetic strategy would enable an efficient and divergent synthesis in the laboratory as well. The risk associated with such a strategy is that a purely chemical synthesis would not possess the enzymatic tools to install oxygenation in a chemo- and site-selective fashion. Such an approach would thus encourage invention of new methods and an exploration of the innate preferences of C–H functionalization in complex terpene hydrocarbon skeletons. The successful eudesmane campaign gave some confidence that such an approach would be viable. Thereafter, a number of examples of two-phase terpene synthesis from our laboratory (ingenol[35–37] phorbol,[38] and thapsigargin[39,40]), as well as from other groups (e.g., Sarpong's phomactin terpenoids,[41] Maimone's *Illicium* sesquiterpenes[42,43], Magauer's mitrephorones,[44] and Maulide's uncargenin C and protobassic acid[45]), have been reported. In addition to those studies, numerous ventures to explore oxidation of terpene scaffolds were initiated, such as ouabain,[46,47] betulinic acid,[48] and polyoxygenated pregnanes.[49]

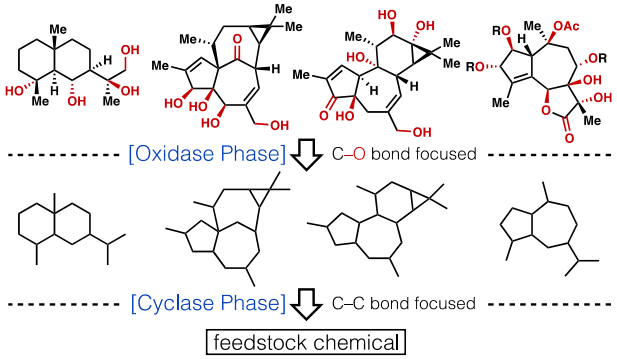

Figure 2. Oxygenated terpene synthesis based on two-phase retrosynthetic logic.

Application of this synthetic strategy to the taxanes, one of the most renowned and complex terpene families, has been an ambitious project in our laboratory for the past decade. Whereas all of our prior studies in this area had an immediate application to pressing medicinal chemistry explorations in collaboration with LEO Pharma and Bristol-Myers Squibb, the Taxol® (**1.1**) venture was purely motivated by fundamental curiosity.[50] In theory, the biomimetic two-phase approach could have the ancillary benefit of enabling a medicinal chemistry approach to taxanes because every oxidation step could allow for a comprehensive structure-activity relationship study of taxanes from low to high oxidation levels. At the outset, the synthetic cyclase phase of the taxane family was accomplished, resulting in syntheses of lowly oxidized

taxanes such as taxadiene (**1.2**, a natural product) and taxadienone (**1.3**, not a natural product).[51,52] It is worth noting that the concise route to enantiopure **1.2** enabled numerous laboratories to study its biosynthesis (nine as of this writing have received samples from our laboratory) despite the existence of PCF-derived sources.[53] Clearly, the completion of an exceptionally concise cyclase phase was a prerequisite to any attempted biomimetic path to **1.1**. In order to explore the hypothesis of whether such a biomimetic strategy would enable an efficient and divergent synthesis of Taxol® (**1.1**), taxane family members[54] at various oxidation levels were deliberately targeted. A unique objective of our two-phase approach to taxanes was to divergently access many natural and unnatural taxane analogs during an oxidative ascent toward Taxol® (**1.1**). The pursuit of such a strategy would ensure that, even if the synthetic approach could not compete with the efficiency of PCF (as already shown by previous practitioners), the divergency would allow access to numerous taxanes and analogs thereof—chemical space which had not been accessed before. Of note, prior medicinal chemistry explorations on **1.1** have relied on semi-synthetic approaches that systematically deoxygenate and functionalize the many oxygenated functionality (Figure 3). These lengthy sequences benefitted from the abundant supply of **1.1**, but were limited by instability of **1.1**,[55] selectivity issues,[56,57] and difficulties of unseemly rearrangements.[58–60]

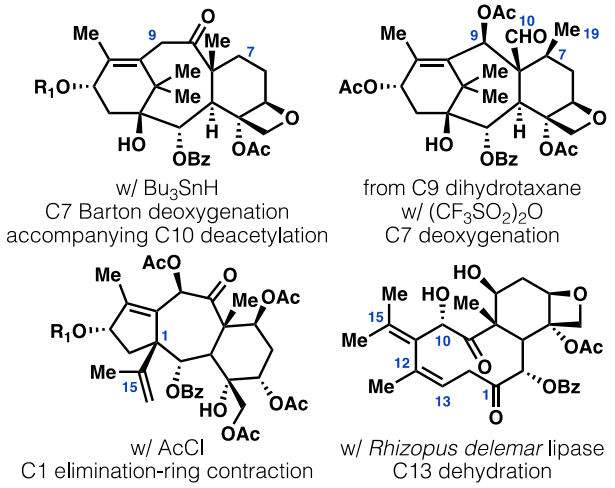

Figure 3. Selected examples of highly oxygenated taxane functionalizations and rearrangements.

1.3 Taxane Oxidase Phase Blueprint and Target Selections

Application of the two-phase strategy to taxane synthesis requires a cyclase phase to a minimally oxidized taxane, followed by at least nine C–O bond-forming steps *en route* to the final target, Taxol® (**1.1**). In Nature, this sequence requires no less than 20 enzymes to accomplish (2 for the cyclase phase, 8 for the oxidations and the rest for functionalizations).[61–63] Although following the exact oxidation sequence of taxane biosynthesis could lead to a greater number of natural products in the oxidative ascent, our targets of interest not only included natural but also unnatural taxanes, and therefore we did not restrict our retrosynthesis to biosynthetic oxidation choreography. Rather than examining all the possible permutations of nine oxidations, shorter-term goals were set where the oxidation steps required for **1.1** were divided into three categories: early, middle, and late oxidation (Figure 4).

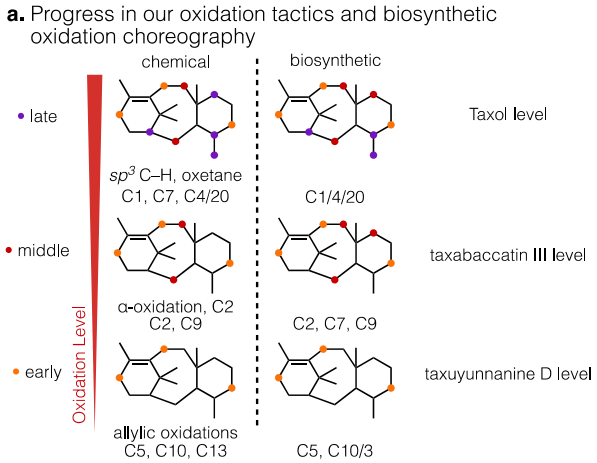

b. Oxidation choreography

	• early	• middle	• late
biosynthesis of Taxol®	5, 10/13	9, 7, 2	1/4/20
original plan for Taxol®	5, 10, 13	2, 9	1, 7, 4/20
taxuyunnanine D	5, 10, 13	–	–
taxabaccatin III	2, 5, 13	9, 10	–
final route for Taxol®	2, 5, 13	1, 7, 10	4/20, 9

Figure 4. (a) A comparison of oxidation choreography between our synthetic plan and biosynthesis. (b) A summary of oxidation choreography.

A salient feature of this approach was the existence of intermediate milestone events that would represent independent accomplishments worthy of Ph.D. theses (to Y.I., N.W., and Y.K.).[64–66] Thus, we set out to achieve two "oxidative milestones" prior to Taxol® (**1.1**):[67] taxuyunnanine D (**1.4**)[68] and taxabaccatin III (**1.5**).[69] The total synthesis targets were chosen such that, if the early oxidation steps were developed, the first taxane target would be reached; if the middle oxidation steps were achieved, the second natural product would be accessed; and if ways to perform the late oxidation steps were uncovered, while keeping the other functional groups intact, Taxol® (**1.1**) would be obtained. The first three carbons oxidized in biosynthesis are C5, C10 and C13. C5 is oxidized prior to C10 and C13 (Figure 4b, *known* oxidation choreography represented with comma) followed by either C10 or C13 oxidation (Figure 4b, *unknown* oxidation choreography represented with forward slash), where ambiguity remains with regards to the oxidation order depending on a specific taxane. These oxidations take place on allylic carbons, which are all functionalized in taxuyunnanine D (**1.4**, Figure 5). For the middle oxidation steps, the synthetic plan adds two functional groups, at C2 and at C9, which are oxidized in taxabaccatin III (**1.5**). At this stage, the planned oxidative choreography and that of Nature differ, but this was not a concern, as an understanding of the feasibility of oxidizing various carbons on the taxane core was sought. Finally, we would add on the last two functional groups, at C1 and C7, as well as forge the functionalized oxetane ring of Taxol®

(**1.1**). In this fashion, the tremendous task of oxidizing eight different carbon atoms was truncated into smaller milestones of three, two and four oxidations (two of which should be a well-precedented task of oxidizing the C4/20 alkene and forming an oxetane).[18] We hypothesized that this stepwise approach would maximize the potential to learn about the innate reactivity of taxanes and ultimately translate to Taxol® (**1.1**). Graphically, the two-phase strategy could be represented as a pyramid-climbing approach as shown in Figure 5, wherein **1.1** would be placed at the apex of an oxidase phase pyramid, **1.4** and **1.5** (black circles) would be embedded as milestones, and both natural and unnatural taxanes in various oxidation levels (gray circles) could be reached in an oxidative ascent toward these molecules.

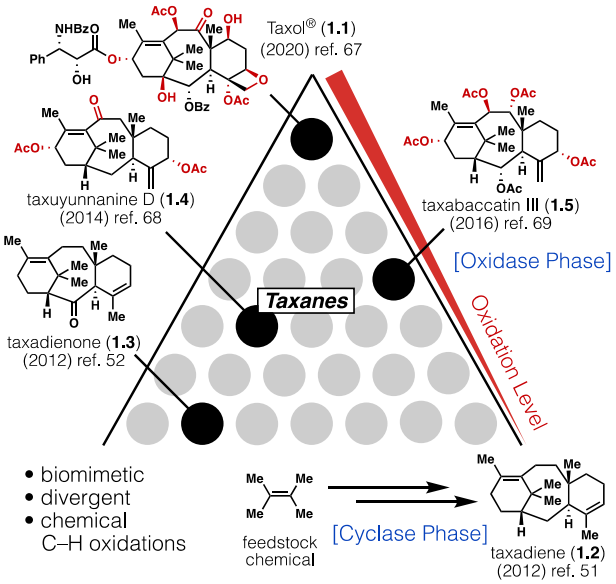

Figure 5. Graphical representation of an oxidase phase approach toward Taxol® (**1.1**) and target taxanes.

1.4 Purpose of this Perspective

Herein, we retrospectively analyze our 13-year synthetic journey to Taxol® (**1.1**) in order to give a perspective on two-phase synthesis logic in its most complex manifestation. It is our hope that the lessons gained here will transcend the customary drama and excitement associated with complex molecule total synthesis. A three-pronged discussion will be introduced here, and elaborated upon after describing the lessons learned from each of the taxane targets.

(a) Significance: What is the value of another chemical synthesis of Taxol® (**1.1**)?

Previous syntheses[17-29] were oriented to answering the question of whether a total synthesis of **1.1** was even possible. Without this curiosity, and considering that the supply issue of **1.1** no longer exists, how can the lessons obtained in this synthetic campaign be useful to others?

(b) Strategy: Was two-phase synthesis logic the most adequate approach to **1.1**?

The advantages of the two-phase logic have already been explored in our group[33,35,38,39] and in others.[41–43] Is the taxane family, and Taxol® (**1.1**) in particular, a suitable platform to test its utility?

(c) Tactics: Did the oxidation choreography laid at the outset need to be revised?

With Nature's biosynthetic oxidase phase, along with the wealth of pre-existing Taxol® (**1.1**) literature,[61,62] a possible blueprint had been laid out.[54] Were the oxidative milestones achieved in the synthesis of taxuyunnanine D (**1.4**)[68] and taxabaccatin III (**1.5**)[69] useful in the synthesis of Taxol® (**1.1**)[67]?

With these questions in mind, we present the overarching lessons learned while overcoming each oxidative hurdle en route to **1.4**, **1.5** and **1.1**. Although the final routes to each of these molecules have been published, the hitherto undescribed failed routes are what allowed us to truly understand the challenges presented by the taxane family, as embodied by the intricacies of oxidation choreography. This 13-year campaign has resulted in a continuous body of in-house knowledge with the initial plan being outlined in 2010[54] and an account of the cyclase phase described in 2012.[52]

Since this perspective discusses in detail the significance, strategy and tactics in the synthesis of **1.1**, many of the routes were exploratory, and the intermediates encountered in those routes were not rigorously characterized (beyond enough data for us to be certain of our assignment). Furthermore, apart from the final synthetic sequences to each of the taxane targets, many of the reaction steps were not quantifiable because they were not conducted in a scale where the yield can be reliably measured. The advantages of certain oxidation choreographies are thus qualitatively assessed, whereas key optimization efforts of key transformations are quantitatively highlighted.

2. Allylic Oxidation of C5, C10 and C13

2.1 Strategic Target Selection: Taxuyunnanine D

Two cyclase phase endpoints, the unnatural taxadienone (**1.3**) and natural taxadiene (**1.2**), were synthesized on gram-scale in 7 and 10 steps, respectively (see Figure 5 for structures).[51,52] Committing to both compounds as ideal entries to the taxane family, including Taxol® (**1.1**) itself, we embarked on the oxidase phase. Since natural taxanes are biosynthetically derived from taxadiene (**1.2**), it was hypothesized that scouting site-selective oxidation tactics from **1.2** might give insights into the natural reactivity of the carbon skeleton. This starting point selection was also desirable from a synthetic point of view because the small number of functional groups present on **1.2** eliminated functional group compatibility issues and streamlined reaction analysis and development.

A widely recognized C2 deoxygenated taxane is taxusin, which has been synthesized by several research groups.[70–74] Many of the tactics developed in the synthesis of taxusin were used to complete the total synthesis of Taxol® (**1.1**).[17,18,23] Another potential target, as described above, is taxuyunnanine D (**1.4**; see Figure 5)[75] because it only has three oxidized carbon atoms, and all of them are

conveniently allylic. This observation is also consistent with the proposed biosynthesis, where oxidation takes place at the allylic positions, first at C5, then at C10, and finally at C13. We reasoned that a synthesis of taxuyunnanine D (**1.4**) would allow us to attain a proof-of-concept in the most concise fashion, and simultaneously gain insight into the innate reactivity of the cyclase phase endpoint **1.2**.

2.2 C5 Oxidation

Even though the biosynthesis of taxanes is well-documented, it was uncertain whether the biosynthetic oxidation choreography would be reproducible by chemical oxidations. Therefore, initial attempts at oxidizing taxadiene (**1.2**) did not target any specific allylic oxidations, but rather probed the vulnerability of its olefins and C–H bonds (Figure 6a) to succumb to oxidation. Sterically unhindered epoxidation reagents such as *m*CPBA preferentially reacted with the electron-rich, bridgehead $\Delta^{11,12}$-olefin to give **2.1** and **2.2**. $^1O_2$ was also selective for the $\Delta^{11,12}$-olefin to give allylic alcohol **2.3**. Kharasch-type conditions, as well as Cr(VI)-mediated oxidation, led to decomposition. Electrophilic selenation gave a diastereomeric mixture at C5 in **2.4**, but reagents to selectively oxidize the selenium atom for selenoxide elimination proved elusive.

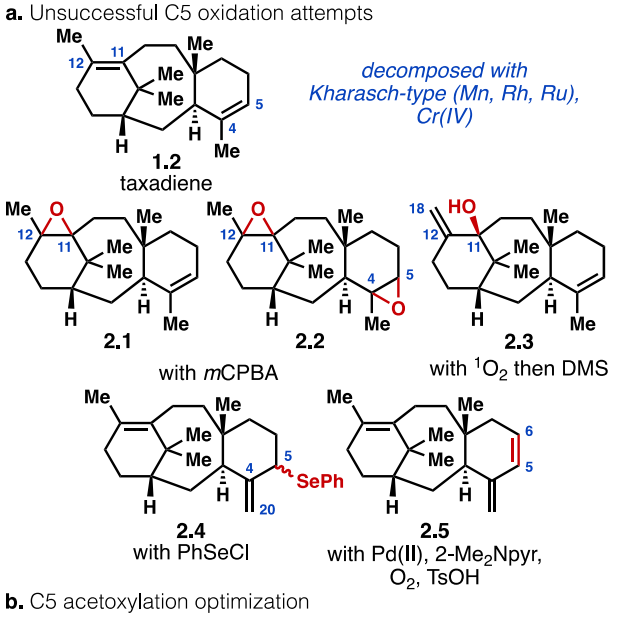

additive	yield [%]
none	35
TMB	41
1,3-dimethoxybenzene	45
anisole	53
N,*N*-dimethylaniline	decomposition

Figure 6. (a) Initial probing of C5 reactivity using taxadiene (**1.2**) as the substrate. (b) The effect of electron-rich arenes for C5 selective acetoxylation.

Finally, Pd(II)-mediated dehydrogenation[76] gave triene **2.5**, but this compound did not prove useful at this stage. Notably, palladium, in conjunction with a sterically demanding oxidant, site-selectively engaged with the $\Delta^{4,5}$-olefin without disruption of the $\Delta^{11,12}$-olefin. Motivated by this outcome, selective C5 oxidation was eventually attained with Pd-catalyzed acetoxylation, leaving the bridgehead olefin intact. Reacting taxadiene (**1.2**) with catalytic $Pd(OAc)_2$ and stoichiometric 1,4-benzoquinone (BQ) in AcOH gave C5 acetate **2.6** as a single diastereomer in 35% yield (Figure 6b).[77–79] In an attempt to determine the identity of the remaining mass balance, the reaction was conducted in an NMR tube using acetic acid-d_4 as solvent and 1,3,5-trimethoxybenzene (TMB) as an internal standard. The time course of the reaction revealed that the sum of the product (**2.6**) and the starting material (**1.2**) steadily declined over time, and there were no discernible peaks in the ^{1}H-NMR to indicate byproducts. Surprisingly, this experiment afforded the product (**2.6**) in slightly improved yield (41%). This led to the discovery that as little as one equivalent of methoxy-substituted electron-rich arenes such as TMB and anisole generates less palladium black, and increased the yield of the acetoxylation to 53%. Also, the yield remained the same irrespective of the catalyst loading.

2.3 C13 Oxidation

Encouraged by C13 allylic oxidation precedents by Kende[80] and Nicolaou,[19] we set our sights on selective C13 oxidation to form enone **2.7** (Figure 7). In seven out of the ten completed syntheses of **1.1**, this oxidation was carried out in high yield at a very late stage.[19,20,24–29] Installing this oxidation at an early stage carries additional risk, as our route to **1.1** would not benefit from many of the learnings of those approaches or the specific electronic characteristics that enabled clean C13 oxidation. Nevertheless, the C13 oxygenation has been shown to be critical for bioactivity and thus, in order to maximize the medicinal relevance of the route, it was earmarked for early installation. Perhaps not surprisingly, treating acetate **2.6** with PCC or CrO_3•3,5-dimethylpyrazole complex (CrO_3•DMP)[81] led to low yields of enone **2.7** alongside epoxide **2.8** and diketone **2.9**, each in *ca.* 30% yield. A number of Cr(VI) reagents were explored in an

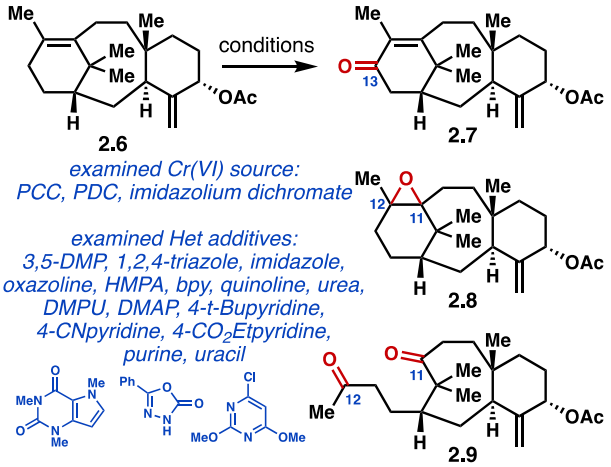

Figure 7. Major side products observed with Cr(VI)-based oxidants, as well as a list of examined additives.

effort to coax the reaction to favor the desired enone **2.7**. PDC and Collins reagent gave similar or worse results.[82] Using CrO_3 with different heterocycles as additives—in an effort to mimic the intramolecular deprotonation believed to be at work with CrO_3•DMP—enabled selective production of epoxide **2.8** or diketone **2.9**, but never furnished the desired enone **2.7**. Substrates that were oxidized in high yield in the past bore the critical C10 functional group, which presumably mutes the reactivity of the $\Delta^{11,12}$-olefin in preference to the desired C13 oxidation. This was an early indication of how distal functional groups on the taxane skeleton dramatically influence each other.

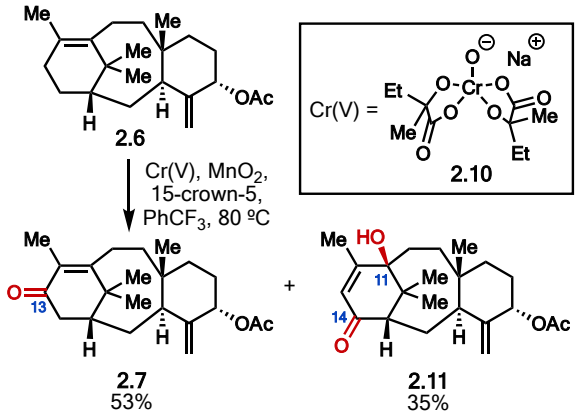

Figure 8. The application of Cr(V) reagent **2.10** for allylic oxidation.

An extensive literature examination identified a hydroxy-acid bound Cr(V) reagent **2.10** (Figure 8), which contains only one Cr=O bond (as opposed to two or three such bonds in Cr(VI) reagents).[83] Although never employed in total synthesis, this study demonstrated the reactivity difference of Cr(V) relative to Cr(VI) with the former eliciting oxidative cleavage of pinacol much slower than the latter.[84] Operating with the hypothesis that the formation of diketone **2.9** would be reduced, Cr(V) reagent **2.10** was prepared and exposed to acetate **2.6**. Gratifyingly, neither diketone **2.9** nor epoxide **2.8** were detected, and the desired enone **2.7** was isolated as the major product. Interestingly, this reaction was now accompanied by a new undesired side product **2.11**.

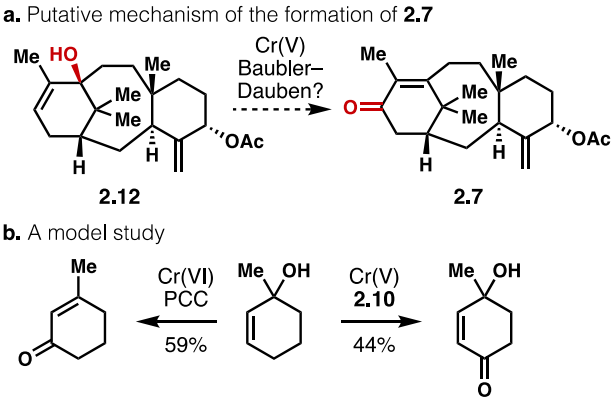

Figure 9. (a) Probing a potential Baubler–Dauben type mechanism. (b) The difference in reactivity between Cr(V) and Cr(VI).

Since this new product suggested that a different mechanism was operating when using Cr(V) reagents versus Cr(VI) reagents, it became critical to elucidate if the desired enone **2.7** was derived, to any extent, from putative tertiary allylic alcohol **2.12** (Figure 9a) as in the Baubler–Dauben reaction.[85,86] However, treatment of **2.12** with Cr(VI) or Cr(V) reagents furnished no trace of enone **2.7**. A model substrate demonstrated the unique reactivity of Cr(V) **2.10** (Figure 9b), which did not effect 1,3-allylic transposition like Cr(VI) reagents (e.g., PCC). Notably, the previously unrecognized utility of this Cr(V)-based oxidant for C–H oxidation has benefitted other recent total syntheses.[87,88]

2.4 C10 Oxidation

As mentioned above, it was not apparent at the outset whether C10 or C13 should be oxidized first, and therefore several C10 oxidation attempts were made prior to C13 oxidation (Figure 10). First, TEMPO-derived oxoammonium salt **2.15** selectively oxidized the C18 position of **2.6** to give **2.14**. Similar selectivity could be induced by a singlet oxygen ene reaction at C11, followed by a unique solvent-dependent 1,3-allylic transposition, giving **2.16**. This C18 alcohol was smoothly eliminated to extend the oxidation state to C10: treatment with MsCl formed diene **2.17** with a $\Delta^{10,11}$-olefin. Unfortunately, this diene could not be isomerized to a $\Delta^{9,10}$-diene despite numerous attempts, presumably because **2.17** has alleviated ring strain. At this juncture, we hypothesized that the C10 oxidation might not be feasible without disrupting the bridgehead olefin, so we committed to oxidizing C13 before C10.

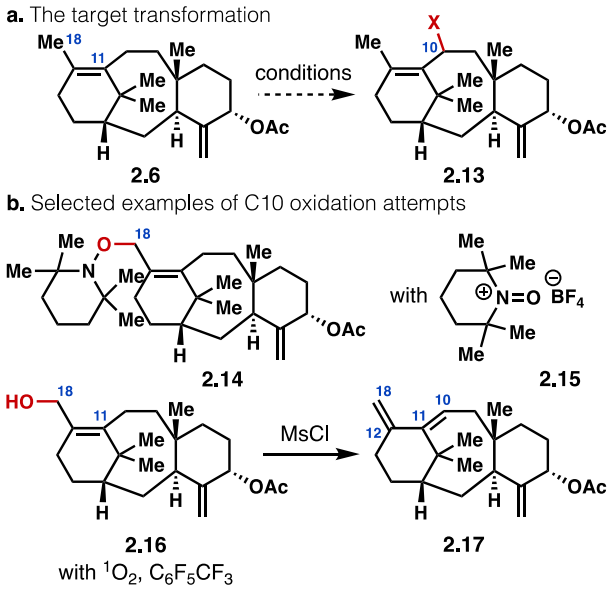

Figure 10. (a) The desired transformation. (b) Unsuccessful C10 oxidation attempts.

Several conditions to oxidize the C10 of enone **2.7** were developed (Figure 11). Treating enone **2.7** with TMSOTf produced a vinylogous(silyl)enol ether (**2.19**), with concomitant C5 acetyl group silylation. Delightfully, this species reacted with NCS to afford allylic chloride **2.20**. Chloride **2.20** was a breakthrough intermediate in the

synthesis of taxuyunnanine D (**1.4**) because the desired C10 oxidation was finally achieved with site selectivity, albeit in two steps from enone **2.7**. In the end, this route was abandoned due to convoluted protecting group manipulations: C5 and C13 functionalities could not be simultaneously liberated as alcohols. A superior approach to C10 oxidation was developed through radical bromination to give **2.21**, which underwent stereoretentive solvolysis upon treatment with AgOTf, even in conjugation with the C13 ketone. The enhanced stability of the C10 radical and suppressed reactivity of the bridgehead olefin by conjugation with the enone guided the reactivity as well as regioselectivity.

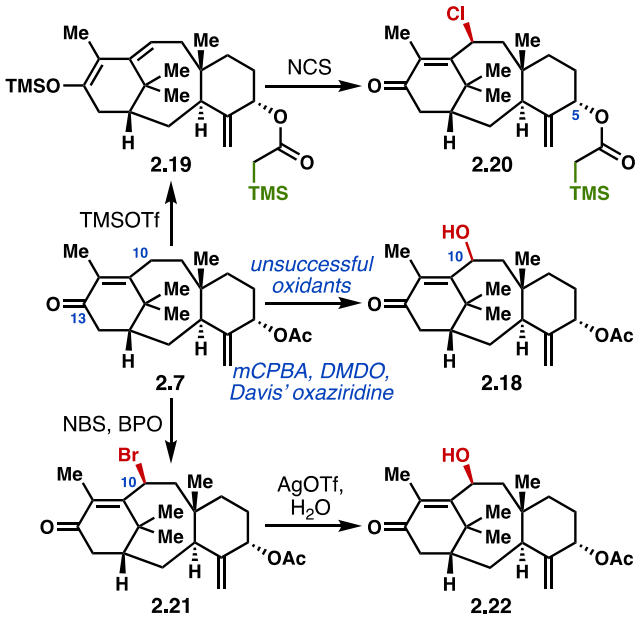

Figure 11. Selective C10 halogenation.

These oxidative explorations established the order of the C5, C10 and C13 site-selective allylic oxidations of the taxane core. Notably, this oxidation choreography is highly analogous to that of biosynthesis, implying that chemical transformations can reproduce the inherent reactivity of taxanes with oxidase enzymes for these early oxidation steps.

2.5 Two-Phase Synthesis of Taxuyunnanine D

Armed with an understanding of the relative reactivities of each allylic position and functional group, taxuyunnanine D (**1.4**) was synthesized as the first demonstration of two-phase taxane synthesis (Figure 12). Thus, taxadiene (**1.2**) was oxidized using a modified Åkermark and Bäckvall type acetoxylation to afford **2.6** as a diastereomerically pure product (step a). C13 oxidation was installed by the aforementioned Cr(V) reagent to give **2.7** (step b). Enone **2.7** was then site-selectively brominated at C10, which was effectively displaced by TESOH in the presence of an Ag(I) salt to install a hydroxyl group and a protecting group simultaneously, minimizing the number of concession steps to **2.23** (step c). Diastereoselective C13 reduction, followed by tandem C5 and C13 acetylation, afforded taxane **2.24** (step d). The final oxidation (step e) was realized with IBX,[89] completing the two-phase synthesis of taxuyunnanine D (**1.4**).

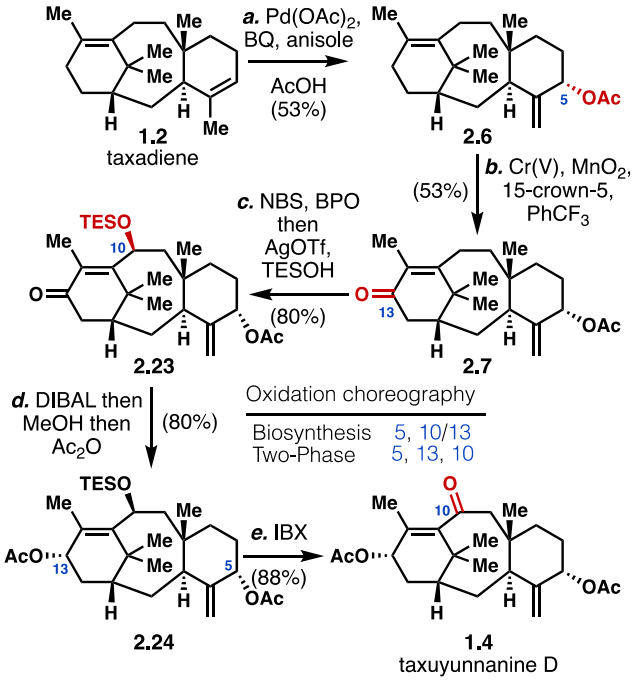

Figure 12. Two-phase synthesis of taxuyunannine D (**1.4**).

3. Introduction of C2 and C9 Oxidation States

3.1 Strategic Target Selection: Taxabaccatin III

The selective oxidation of C5, C10 and C13 opened a seemingly clear path toward the next stage of operations needed to access higher taxane oxidation levels. The cyclase phase had led to two taxanes, taxadiene (**1.2**) and taxadienone (**1.3**),[51] the latter of which is oxidized at C2, much like other taxane natural products. However, there is no reported analog of taxuyunnanine D (**1.4**) bearing oxidation at C2. With reliable oxidation methods for C5, C10 and C13 in hand, the next objectives were determined (Figure 13): (i) installation of oxidations at C5, C10 and C13 with a C2 oxidized functionality in place; (ii) stereocontrolled C2 installation; (iii) C9 oxidation; and (iv) stereoselective C9/10 diol formation. With these tactical goals in mind, taxabaccatin III (**1.5**)[90] was chosen as the next target, which posed additional stereochemical challenges at C2, C9 and C10. The fact that many natural taxanes share this C9/10 *trans*-diol pattern underlined the importance of developing a tool to stereoselectively install such a motif.

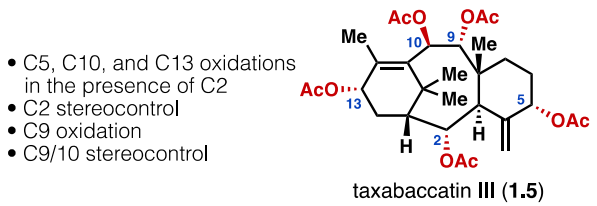

Figure 13. The next targeted taxane and associated challenges.

3.2 The $\Delta^{9,10}$-Olefin as a C9/10 Diol Synthon: Taxatriene

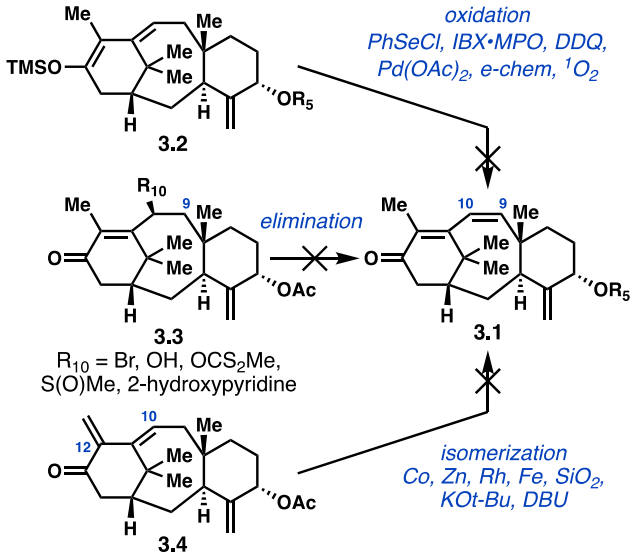

Figure 14. $\Delta^{9,10}$-olefin installation attempts. MPO, 4-methoxypyridine *N*-oxide.

At the outset, tremendous efforts were made to generate a taxane containing the $\Delta^{9,10}$-olefin moiety (**3.1**; Figure 14). The goal was to oxidize this olefin to furnish the key C9α and C10β motif in a minimal number of transformations. These efforts can be categorized in three approaches: (i) oxidation of vinylogous silyl enol ether **3.2**; (ii) elimination of a C10 functional group from **3.3**; and (iii) isomerization of diene **3.4**. Unfortunately, none of these approaches afforded the desired $\Delta^{9,10}$-olefin. The difficulty associated with the $\Delta^{9,10}$-olefin installation stems from the strained nature of the olefin (which could lead to rapid isomerization to **3.4**) and poor orbital alignment for the desired E2 elimination (for *anti,* or even *syn*, elimination).

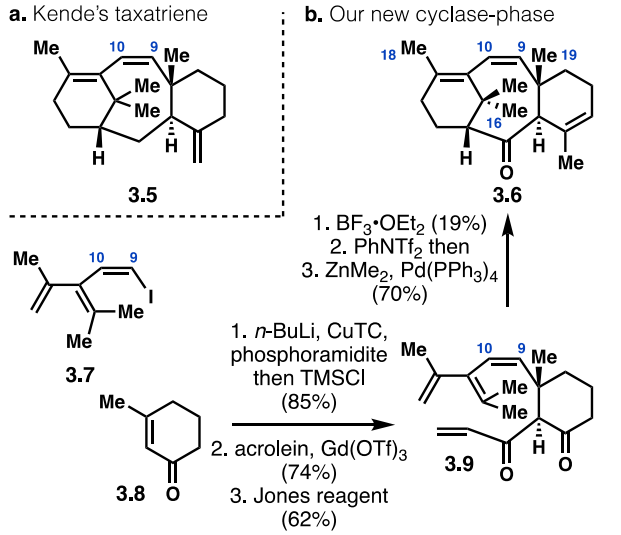

Figure 15. (a) Kende's taxatriene. (b) A new cyclase phase designed to install the $\Delta^{9,10}$-olefin.

These observations were consistent with Kende's synthetic approach to taxatriene (**3.5**), where the $\Delta^{9,10}$-olefin had been incorporated prior to the skeletal construction (Figure 15a).[80] This inspired the development of a new cyclase phase with a pre-installed $\Delta^{9,10}$-olefin (Figure 15b). The eventual synthesis of triene **3.6** started from **3.7** and **3.8** by following a similar procedure to the cyclase phase of taxadienone (**1.3**).[51,69]

Considering the strained nature of the $\Delta^{9,10}$-olefin, one might assume it to be fairly reactive. To our dismay, this was not the case, and oxidation of this olefin turned out to be an extreme challenge as well. Figure 16 depicts a number of examined substrates that contain a $\Delta^{9,10}$-olefin. All but the last set of substrates decomposed or were left unreacted under a number of different oxidation conditions (e.g. *m*CPBA, DMDO, OsO_4, TFAA/H_2O_2). The remarkable recalcitrance of the $\Delta^{9,10}$-olefin to react with any oxidant can be explained in hindsight by examination of the X-ray crystallographic structure (**3.10**, Figure 16). One can see the steric hindrance created by the C16, C18 and C19 methyl groups, as well as the C7 methylene group. These four carbons effectively confine the $\Delta^{9,10}$-olefin inside the taxane skeleton.

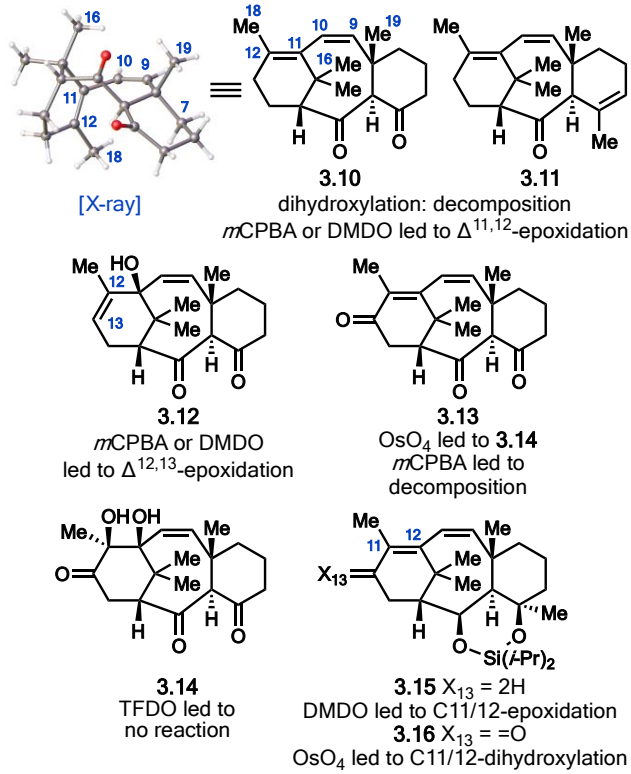

Figure 16. $\Delta^{9,10}$-olefin oxidation attempts. Crystallographic data for compound **3.10** has been deposited with the Cambridge Crystallographic Data Centre as no. CCDC-1435376.

In fact, only a few compounds (e.g., **3.17**; Figure 17) exhibited a reactive $\Delta^{9,10}$-olefin, but these were only reactive after a Meinwald rearrangement of the $\Delta^{11,12}$-epoxide, forging a rearranged skeleton with a C10/12 bond. Although the $\Delta^{9,10}$-olefin was an appealing retron for the oxidation of C9 and C10, the oxidase phase starting from taxatriene **3.6** was abandoned after these extensive efforts.

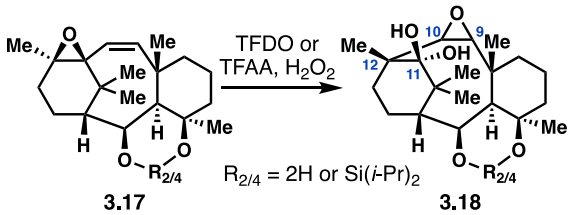

Figure 17. Unexpected skeletal rearrangement occurred during an $\Delta^{9,10}$-olefin oxidation attempt.

3.3 C2 Alcohol Derails the Plan for C5 Oxidation

The unreactive nature of the $\Delta^{9,10}$-olefin guided us to pursue a different oxidation choreography, where C9 could be installed in an oxidation relay from the C10 ketone, a strategy employed in much of the prior art.[18,20] As our current tactics necessitated C13 oxidation prior to C10, it was sensible to carry out all allylic oxidations and then address the C9 challenge at the very end. Originally, there were no major concerns of executing C5, C10 and C13 oxidations with the C2 oxidized functionality present. Oxidation choreography was deemed to be the only issue as the targeted taxane (**1.5**) contained as many as five secondary alcohols to be differentiated.

We soon realized that the Bouveault–Blanc reduction[91] that worked well to give the desired C2 α-alcohol from taxadienone (**1.3**) was highly substrate-specific, and produced the β-alcohol in most cases. Therefore, stereoselective C2 reduction had to be performed at the very beginning of the synthesis. Compounding this issue was that attempted Pd-catalyzed C5 acetoxylation only led to C2/20 ether formation (**3.21**), even with an alcohol protecting group (**3.20**; Figure 18). This THF ring could not be opened under any examined conditions, necessitating the development of a new selective oxidation of C5 in the presence of C2 functionality.

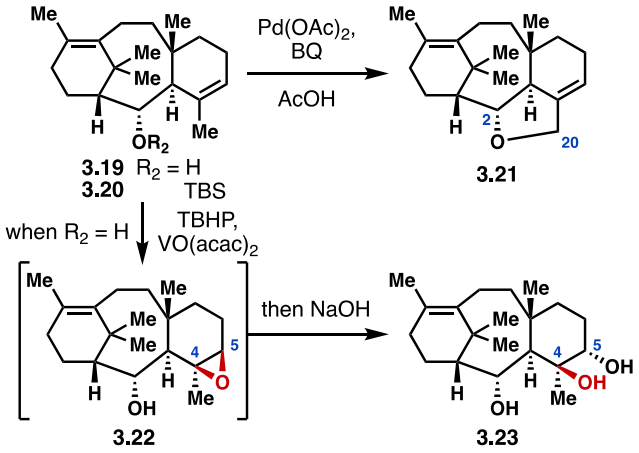

Figure 18. Undesired THF ring formation to give **3.21**, leading to further examination of C5 oxidation methods.

Ultimately, the originally cumbersome C2 alcohol was utilized in a vanadium-catalyzed directed epoxidation of the $\Delta^{4,5}$-olefin, leaving the electron-rich $\Delta^{11,12}$-olefin intact.[92] The resulting C4/5 epoxide (**3.22**) was directly converted to a C5 α-hydroxyl group (**3.23**) in a regio- and stereoselective-manner with NaOH. Notably, the C4 *tert*-alcohol served as a quasi-protecting group for the $\Delta^{4,20}$-olefin (via dehydration).

3.4 Setting the C9α, C10β Diol Oxidation Pattern Toward Taxabaccatin III

Fortunately, the C13 and C10 allylic oxidations employed for the synthesis of taxuyunnanine D (**1.4**) could be smoothly adopted to the synthesis of **3.24** (Figure 19), a C2 α-alcohol version of **1.4**. This set the stage for the C9 oxygenation. Unlike Holton and Takahashi's substrates,[18,26] the C10 enone did not undergo α-oxidation with $(PhSeO)_2O$. After a large array of base, oxidant and temperature screening, a combination of MoOPh[93] and $LiNEt_2$ was identified to be the optimal reagent choice to give **3.26**. Numerous reduction conditions from **3.26** to the corresponding C9α, C10β diol (**3.25**) were examined, however the desired product was not observed. Instead, the C9α, C10α diol was often produced if the starting material did not completely decompose. This undesired stereoselectivity was consistent with the scarce literature precedent,[94] stemming from the caged nature of taxanes. C9/10 redox rearrangement (**3.26** to **3.29**)[18] was also unsuccessful despite the precedent on similar substrates. It is possible that the unique B ring conformation of **3.26** prevented these redox manipulations, which led to the Cu-mediated preparation of diketone **3.27**, possessing a different hybridization pattern and a potentially different conformation. The use of $Cu(OAc)_2$ is known in the context of α-hydroxy ketone oxidation, but had not been used before in approaches to taxanes. After an extensive screening of reductants, the desired stereoselectivity of C9 reduction was attained with a bulky ate-complex, LiAlH(O*t*-Bu)*s*-Bu_2,[95] to afford **3.28** (isolable). Upon

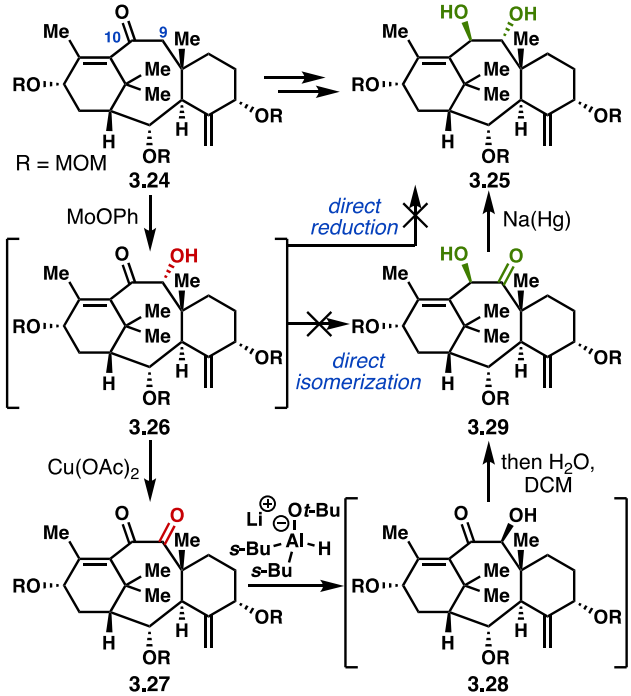

Figure 19. C9 and C10 redox sequence to the C9α, C10β motif.

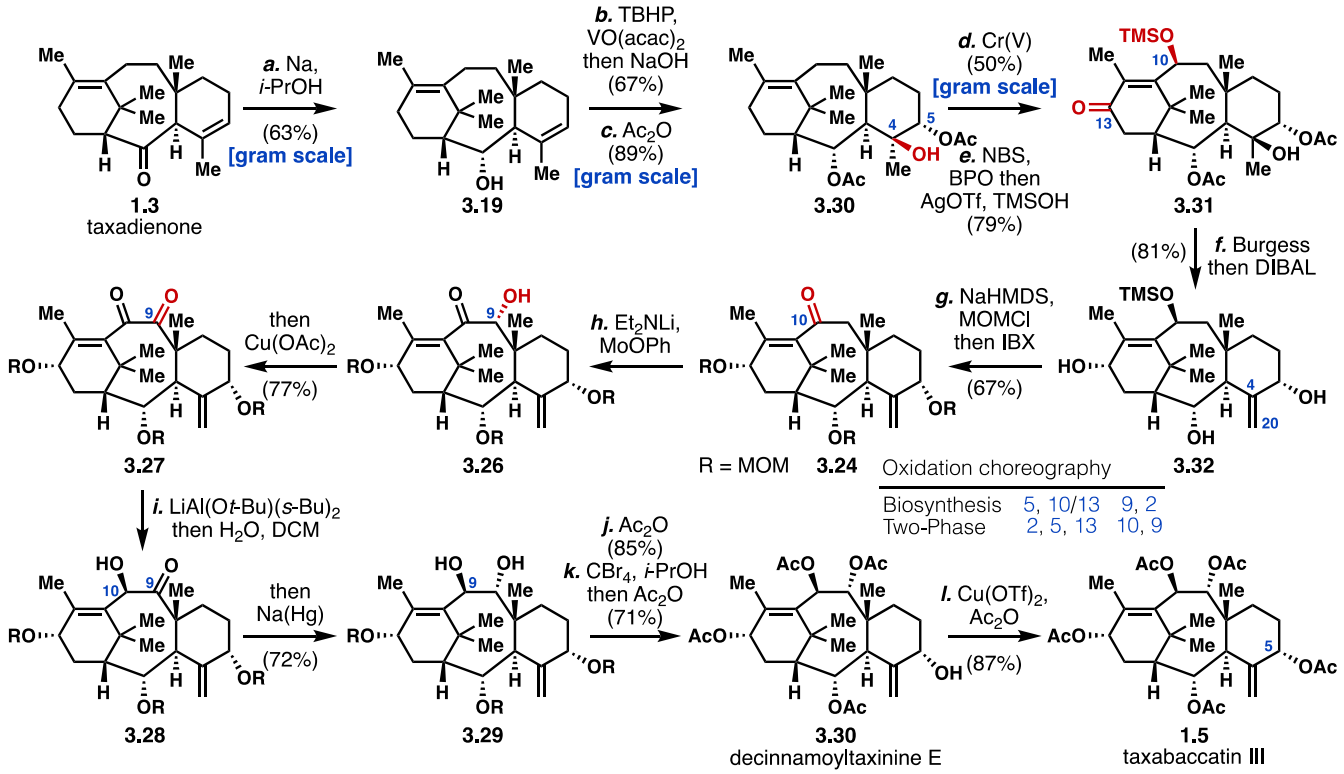

Figure 20. Two-phase synthesis of decinnamoyltaxinine E (**3.30**) and taxabaccatin III (**1.5**).

quenching the reaction with DCM/water, this keto alcohol successfully isomerized to **3.29**. The final thermodynamic reduction of the C9 ketone using Na (Hg) established the key C9α, C10β diol moiety to give **3.25**. This redox manipulation was an essential tactic to complete the middle-stage oxidations to arrive at the taxabaccatin III (**1.5**) oxidation level.

3.5 Two-Phase Synthesis of Decinnamoyltaxinine E and Taxabaccatin III

The reconnaissance gained from the prior sections enabled the completion of natural taxanes decinnamoyltaxinine E (**3.30**) and taxabaccatin III (**1.5**) as shown in its full form in Figure 20. The route commenced with taxadienone (**1.3**), and the stereochemistry of C2 was set at the outset (step a). Teachings from the synthesis of **1.4** were used to install all the allylic oxidations (steps b-g), after which the correct oxidation pattern at C9/10 was installed as described in the previous section (step h, i). Finally, deprotection and acetylation furnished two natural taxanes, decinnamoyltaxinine E (**3.30**)[96] and taxabaccatin III (**1.5**).

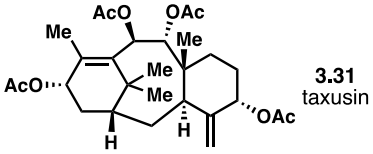

Figure 21. The structure of taxusin (**3.31**).

Taxanes in this oxidation level (**3.30** and **1.5**) had never been pursued as a target of total synthesis, while taxusin (**3.31,** Figure 21), a taxane with one oxidation level lower than **3.30** and **1.5**, has been a popular synthetic target. It has culminated in numerous studies and three total syntheses from the groups of Holton (49 steps, chiral pool),[71] Paquette (40 steps, chiral pool),[73,74] and Kuwajima (28 steps, enantioselective).[72] These target-oriented approaches demonstrated the feasibility of chemically accessing a single taxane. On the other hand, the two-phase strategy was advantageous from the perspective of efficiency as well as divergency. Even though the two-phase disconnection is linear by nature, taxanes **3.30** and **1.5** were prepared in 19 steps from commercially available feedstock chemicals, which is significantly shorter (even with the higher complexity of these targets compared to **3.31**). In addition, the two-phase strategy assembled the entire taxane skeleton at as early as step 7 and installed the C13 oxidation state, an essential oxidation for bioactivity, at step 11. In contrast, prior art completed the carbon skeleton construction at a later stage (Holton: 49, Paquette: 33, Kuwajima: 24).

4. Oxidation Attempts for C1 and C7

4.1 Directed C7 Oxidation Attempts

At this juncture, in 2015, there was an overexuberant feeling that the remaining oxidations needed to access Taxol® (**1.1**) would be straightforward to achieve. After all, nearly all of the key carbon atoms needed to finish **1.1** were either at the correct oxidation state or poised for oxidation: functional groups at C2, C5, C9, C10 and C13 were established, which left "only" two oxidations at C1 and C7 (as well as constructing the functionalized oxetane ring). C7 oxidation was addressed first because methylene C–H oxidation is significantly more challenging than the

comparatively electron-rich methine C–H oxidation (C1). Difficulties of C7 oxidation include: (i) selective methylene C–H oxidation (without oxidizing C6); (ii) steric hindrance presented by the neighboring quaternary center (C8); and (iii) functional group compatibility in the presence of a strong oxidant. Around that time, our group published a modified variant of Schönecker's oxidation[97] for the total synthesis of steroids (**4.1**),[49] which led us to pursue directed methylene C–H oxidation (**4.2**; Figure 22). The target C7 C–H bond seemed to be perfectly aligned with the C9 carbonyl group, a spatial relationship that is geometrically similar to **4.1**.

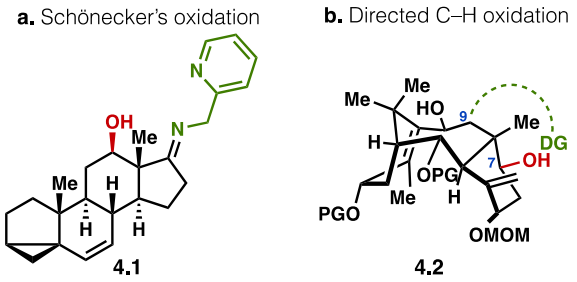

Figure 22. (a) Schönecker's oxidation on an intermediate for C12 oxidized steroid synthesis. (b) The desired outcome of a C9 directed C7 oxidation product.

Taxanes bearing various oxidation patterns with different protecting groups (**4.3**) were assembled (Figure 23a) following the previously developed oxidase phase for decinnamoyltaxinine E (**3.30**) and taxabaccatin III (**1.5**). Our initial approach started by examining oxime/imine-directed C–H oxidation (Figure 23b) inspired by seminal work by Baldwin[98] and Schönecker.[97] Unfortunately, C9 ketone condensation to give an imine or an oxime were unsuccessful, probably because the antibonding orbital of the C9 ketone is buried in the concave face of the taxane core. We then examined a Neber rearrangement[99] by condensation of an oxime on the C10 ketone to introduce nitrogen-based functionality at the C9 position. However, the C10 ketone was similarly unreactive, likely for the same reason. Simple α-amination was also examined, however, the desired reaction did not take place, instead returning the starting material despite the ease of engaging C9 in α-oxidation.

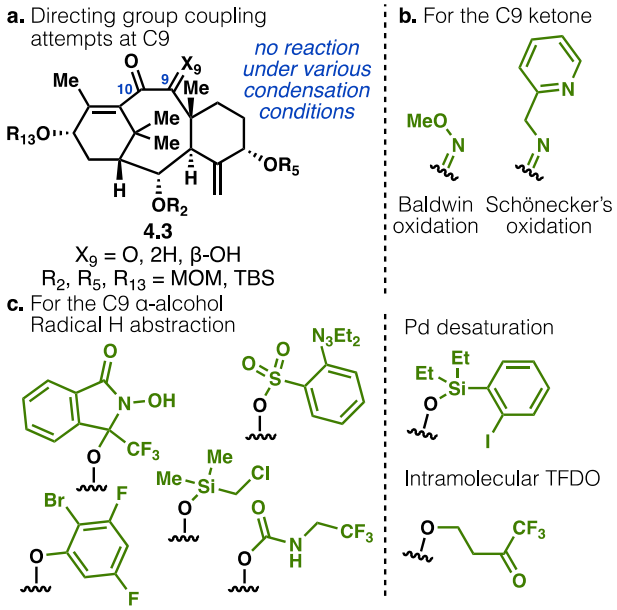

Figure 23. Substrates of interest with a directing group on C9 that ultimately could not be synthesized. (a) A representative structure. (b) Attempted ketone-based condensations. (c) Attempted substitution of the α-alcohol.

The observed inertness of this ketone, as with the $\Delta^{9,10}$-olefin (Section 3.2), suggested that these positions on the taxane skeleton are simply too hindered. Therefore, a C9 alcohol, which equates to a one-atom extension of the reaction site away from the taxane core, was introduced for appendage of a directing group. A variety of directing groups were considered (Figure 23c), with the following transformations in mind: *O*-centered radical C–H abstraction,[100] remote desaturation,[101] palladium-mediated sp^2-radical generation,[102] electron-poor sp^2-radical generation, a Hofmann-Löffler-Freytag (HLF) type reaction,[103] Stork's homologation reaction[104] and intramolecular TFDO.[105] However, due to the low nucleophilicity of the C9 alcohol, stemming from possible hydrogen bonding with the neighboring C10 ketone, inductive effects, and steric hindrance, the C9 α-alcohol gave no reaction with all the depicted directing groups under various conditions.

Directing group installation on the C9 alcohol was not a complete failure, as some small and reactive electrophiles coupled with the C9 alcohol (Figure 24). Pyruvate **4.4**[106] and silane **4.5**[107] could be formed as intramolecular dioxirane and iridium-catalyzed C–H silylation precursors, respectively, although the subsequent C–H oxidation did not proceed in either case. Even directed amination[108,109] was examined with a sulfamate ester in the presence of the rhodium catalyst. To our surprise and

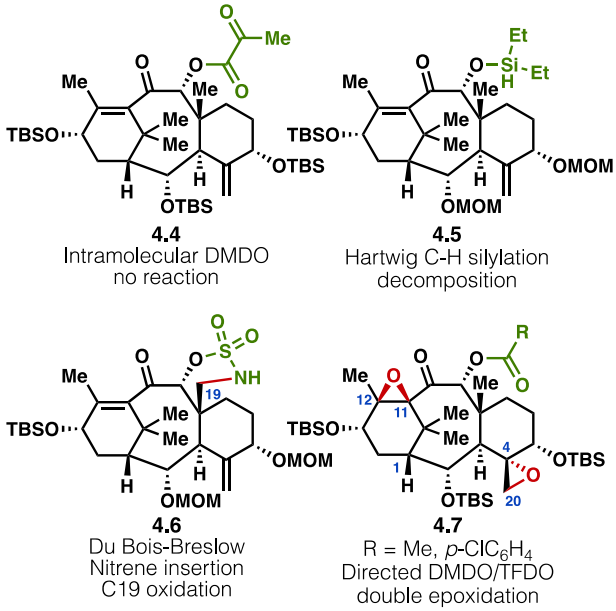

Figure 24. Substrates that were successfully prepared, but with which C7 oxidation was unsuccessful.

dismay, nitrene insertion took place at the C19 methyl over the C7 methylene to give **4.6**. The sterics controlled the selectivity over the electronics, demonstrating the congested environment around the C7 C–H bond.

We envisioned that the unreactive nature of the C7 position could be overcome by using one of the strongest chemical oxidants known, TFDO. Acetate and *p*-chlorobenzoate, which are known to direct TFDO,[110] were appended onto the C9 hydroxyl group. Disappointingly, these compounds did not yield the desired C7 oxidized product with TFDO, but instead epoxidized the $\Delta^{4,20}$- and $\Delta^{11,12}$-olefins to give **4.7**, followed by gradual decomposition. Notably, it was alarming that the C1 oxidation did not happen in the presence of TFDO since we optimistically assumed that oxidizing the only accessible tertiary C–H bond (at C1) would be relatively straightforward.

At this juncture, we concluded that directed C7 oxidation was not viable due to several confounding observations: (i) steric hindrance around the C9 ketone/alcohol prevented the appendage of directing groups; (ii) steric hindrance around C7 blocked the approach of directing groups and oxidants; (iii) substrates exhibited instability to harsh oxidation conditions; (iv) poor material throughput; and (v) highly oxidized substrates had more electron-deficient C–H bonds, and thus might not be ideal substrates for C–H oxidation.

4.2 Directed C1 Oxidation Attempts

Oxidation of the C1 position proved similarly problematic. Some challenges of this oxidation included: (i) the hindered and conformationally restricted nature of the *sp*^{3} bridgehead C–H bond; (ii) a skeletal rearrangement that occurs when generating cations and radicals;[59,111] and (iii) functional group compatibility. The inertness of the C1 C–H bond to TFDO hydroxylation (see **4.7** in Figure 24) raised concerns regarding the feasibility of C1 oxidation. We hypothesized that this could be further examined by creating a kinetically biased oxidizing environment around C1 using a directing group (Figure 25a). Our initial studies on directed C1 oxidation commenced with a model substrate residing in a lower oxidation state, taxadienone (**1.3**). Much like the C9 ketone condensation, however, the sterically hindered C2 ketone did not react with any nucleophiles (Figure 25b). Notably, deprotonation of the C1 bridgehead proton failed, indicating that the bridgehead enolate cannot be formed (the C3 C–H is also sterically inaccessible). In contrast, Holton[17] and Wender[16,21] carried out C1 oxidations using C2 ketones in their syntheses, which was only possible because the full taxane skeleton was constructed after the α-oxidation step. A number of directing group installations with the C2 α-alcohol substrate (**3.19**) were also precluded due to its poor nucleophilicity (Figure 25c).

As with the C9 alcohol, some directing groups could be mounted on the taxane C2 alcohol: successfully generated substrates are shown in Figure 26a. Although most transformations starting with these substrates resulted in no reaction, unproductive reaction or substrate decomposition, DuBois-Breslow[108,109] nitrene insertion chemistry chemoselectively furnished a C1 aminated product in the presence of an olefin and allylic C–H bonds with both carbamate and sulfamate tethers (**4.17** to **4.18**; Figure 26b). The C1 aminated scaffold **4.18** could be prepared in a reproducible manner; therefore, carbamate deprotection was examined to replace this amino group with a hydroxyl group via Barton deamination,[112] even though this tactic could potentially lead to C1 radical-driven skeletal rearrangements.

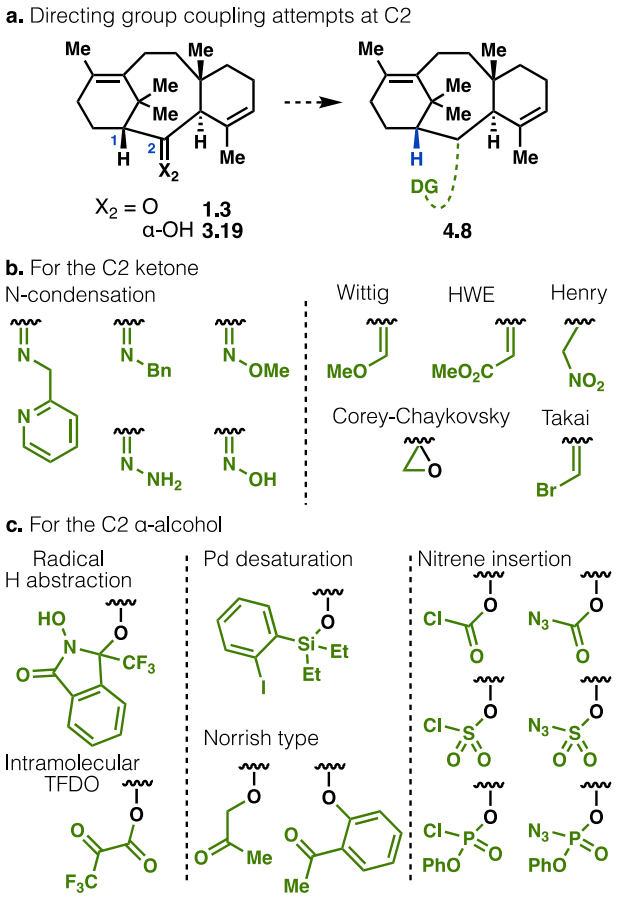

Figure 25. Substrates of interest with a directing group on C2 that ultimately could not be synthesized. (a) A representative structure. (b) Attempted ketone-based condensations. (c) Attempted functionalization of the α-alcohol.

Numerous conditions and approaches, including hydrolysis, reduction, organometallic reagent addition, formation of a diazo species, *O*-alkylation, *N*-alkylation and thiocarbamate formation, were examined for carbamate removal; however, the ring-opened product was never observed. Luckily, Schwartz's reagent was discovered to be a potent reductant for **4.18** to produce oxazoline **4.22**, while even $LiAlH_4$ did not react with **4.18**. Unfortunately, compound **4.22** could not deliver the free C1 amine. The observation that even **4.22** does not undergo deprotection led to the hypothesis that formation of a putative tetrahedral intermediate is unfavored due to a steric clash with the taxane backbone. In conclusion, the strategy of directed C1 oxidation was abandoned because of: (i) sterically challenging functionalization of the C2 ketone and alcohol; (ii)

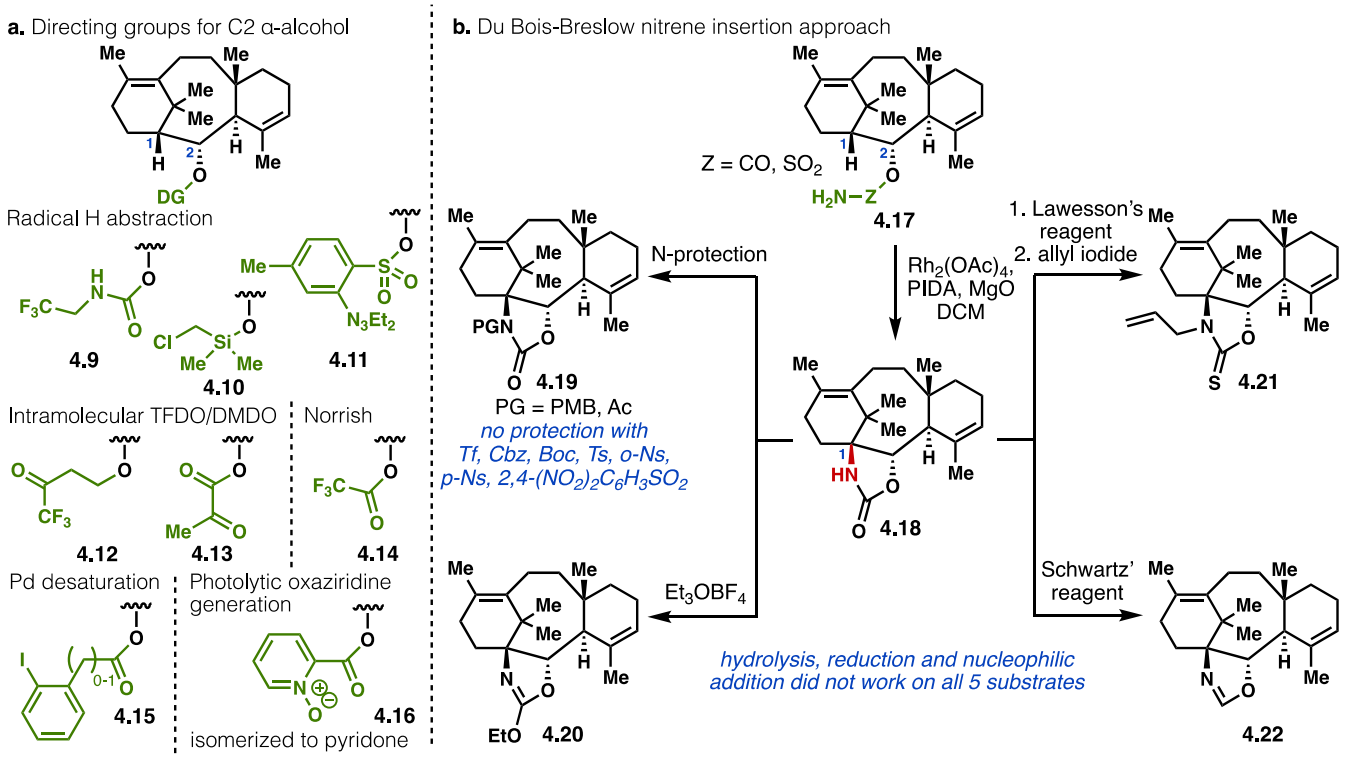

Figure 26. (a) C2 α-alcohol-based substrates that were successfully prepared, but with which the subsequent C–H oxidation was unsuccessful. (b) C2 directed C1 amination, and subsequent attempts to render the cyclic carbamate useful for C1 oxygen atom installation.

substrate instability to harsh oxidation conditions; and (iii) potential skeletal rearrangement issues upon radical and cation generation at C1.

4.3 Glimpse of C1 Oxidation, Leading to a New Oxidase Phase

Directed C–H oxidation approaches for both C7 and C1 did not work, possibly because directing groups could not adopt a suitable geometry relative to the target C–H bond. Indeed, 1,2-diol synthesis methods via directed C–H oxidation reactions are very scarce in the literature.[113] Therefore, small and strong oxidants such as DMDO and TFDO were examined, but this time without direction from C2. Encouragingly, there is compelling literature precedent by Oritani[114] that conducted C1 C–H oxidation on a highly oxidized taxane **4.23** (Figure 27a). One of the most advanced (oxidized) substrates, **4.26**, was prepared and subjected to the same conditions as described in the literature. Surprisingly, despite the structural similarities between **4.23** and **4.26**, C1 oxidation was not observed, but instead the double epoxidation product (at the $\Delta^{11,12}$- and $\Delta^{4,20}$-olefins), **4.27**, was obtained as a single diastereomer (Figure 27b). The C11/12 bridgehead epoxidation was worrisome because: (i) the $\Delta^{11,12}$-olefin is a so-called "hyperstable" bridgehead alkene,[115,116] which is actually not strained and is expected to be stable; (ii) the epoxide might inductively deactivate the C1 C–H; and (iii) converting the C11/12 epoxide back to a bridgehead olefin would take extra steps and might cause chemoselectivity issues. Disappointingly, the desired C1 oxidation product was never observed even after extensive screening (Figure 27c). The overall reactivity trend could be summarized as follows: (i) TFDO was too harsh for this class of substrates; (ii) even *in situ* generated TFDO (i.e., with a lower effective concentration) was too harsh; (iii) C1 was inductively deactivated by the bridgehead epoxide, as well as by the oxygen functionality at C2, C10, and C13; (iv) C13 was gradually oxidized to the ketone even with TBS protection after 15 h (at room temperature with DMDO); (v) $\Delta^{4,20}$-olefin epoxidation was rapid (<1 h at room temperature with DMDO) while C11/12 epoxidation became noticeable after 15 h; (vi) C10 and C13 silyl ether protecting groups seemed to kinetically protect the bridgehead olefin from epoxidation; and (vii) neither sterics nor electronics of the C2 protecting group influenced the outcome. Two differences exist between our substrate **4.26** and Oritani's substrate **4.23**: the oxidation state of the C2 and C7 positions. We assumed that the C7 substituent would not affect the C ring conformation, and that it would only present a minor electronic influence on C1 reactivity, which was consistent with the fact that Oritani's substrate had electron-withdrawing acetyl groups on all hydroxyl groups distal to C1. This led us to conclude that the presence of the C2 α-alcohol was sterically or electronically detrimental to C1 reactivity. The simplest way to validate this idea was to explore the oxidation of C2 *epi* taxane **4.28**, which was synthesized by intentionally reducing the C2 ketone to the wrong β-stereochemistry (Figure 27d).

To our delight, C1 oxidized product **4.29** was observed for the first time, albeit in trace amounts. The β-stereochemistry of the alcohol could have simply reduced the sterics around the C1 C–H bond. It is

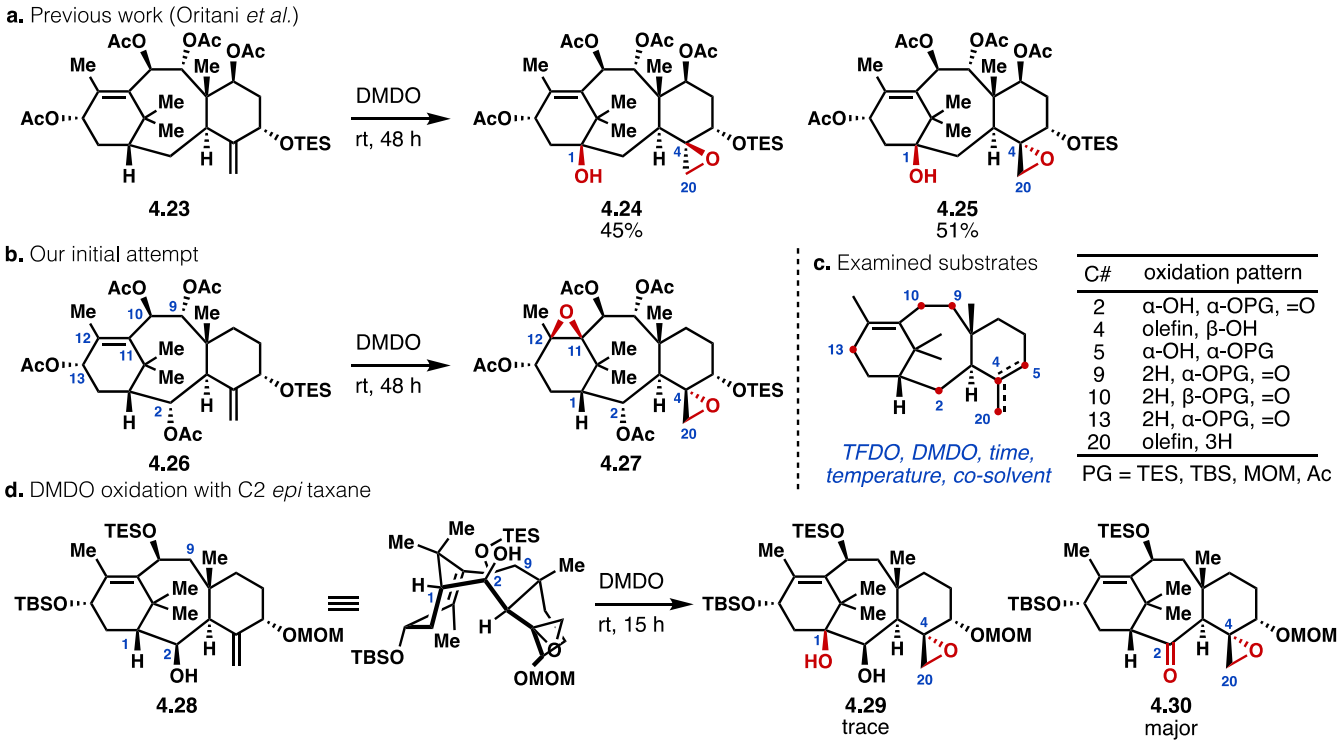

Figure 27. (a) Oritani's seminal C1 oxidation report. (b) Our initial DMDO oxidation attempts on a C2α substrate. (c) Summary of examined substrates. (d) The first successful C1 oxidation enabled by a C2β substrate.

unlikely that a hyperconjugative effect plays an essential role because the dihedral angles look very similar in both diastereomers. Hydrogen bonding from the C2 β-hydroxyl group could affect the reaction rate, whereas the more solvated C2 α-alcohol might misdirect DMDO and sabotage the desired reactivity.[117] Scalable production of **4.28** was therefore necessary to optimize the C1 oxidation and pursue Taxol® (**1.1**), however C2 ketone reduction to give the C2 α-stereochemistry in the first step of the oxidase phase was considered to be non-ideal. Therefore, it was decided that a new oxidase phase would be designed to streamline the overall sequence and improve the material throughput. Part of this analysis included delaying the installation of C9 oxygenation until after C1 was present.

This new oxidase phase, outlined in Figure 28, delivered important clues needed for the ultimately successful route to **1.1**. The synthesis commenced with taxadienone (**1.3**), which was site-selectively oxidized at C5 employing an Åkermark-Bäckvall palladium-catalyzed C5 allylic acetoxylation that was previously employed for taxuyunnanine D (**1.4**) synthesis.[68] C2 ketone reduction and C5 MOM protection were then realized with high selectivity to give **4.32**. The C13 and C10 oxidation steps proceeded using the previously developed conditions to give **4.34**, concomitantly re-oxidizing the C2 alcohol back to the ketone. Stereoselective 1,2-reduction at C13, TBS protection, and C2 reduction with $LiAlH_4$ afforded intermediate **4.28**. Protection of the C2 β-alcohol was examined to suppress the competitive C2 oxidation that takes place during the C1 oxidation; however, the C2 β-alcohol of **4.28** was virtually inaccessible, as it was buried between two methyl groups (C16 and C19). We then made use of the kinetic isotope effect (KIE) to serve as the smallest oxidation-resistant protecting group for the alcohol.[118,119] The use of KIE to control reactivity is a tactic that has been employed in several syntheses.[120–123] Indeed, $LiAlD_4$ reduction product **4.37** subdued the undesired C2 oxidation, thereby kinetically favoring the desired C1 oxidation product (**4.39**) upon treatment with DMDO. However, use of TFDO on compound **4.37** did not yield the desired product and instead led to decomposition, indicating that the reagent and the substrate needed to be precisely matched to realize this objective.

4.4 Challenging Stereoselective C2 Reduction in the Presence of C1 Alcohol

Before installing the missing oxidations at C7 and C9, the C2 alcohol stereochemistry needed to be corrected since it had been intentionally installed incorrectly to achieve C1 hydroxylation. Ley–Griffith conditions readily oxidized C2 to ketone **4.40**, which was then subjected to reduction conditions (Figure 29a). Unsurprisingly, hydrides and protons were exclusively delivered from the α-face to afford C2 β-alcohols as a single diastereomer. The β-face of the C2 ketone in **4.40** was completely blocked by the methyl groups at C16 and C19, as well as by the C10 OTES group. Therefore, hydrogen atom delivery from that face was impossible despite the fact that the intermediate α-ketyl radical should thermodynamically favor the α-configuration. Numerous

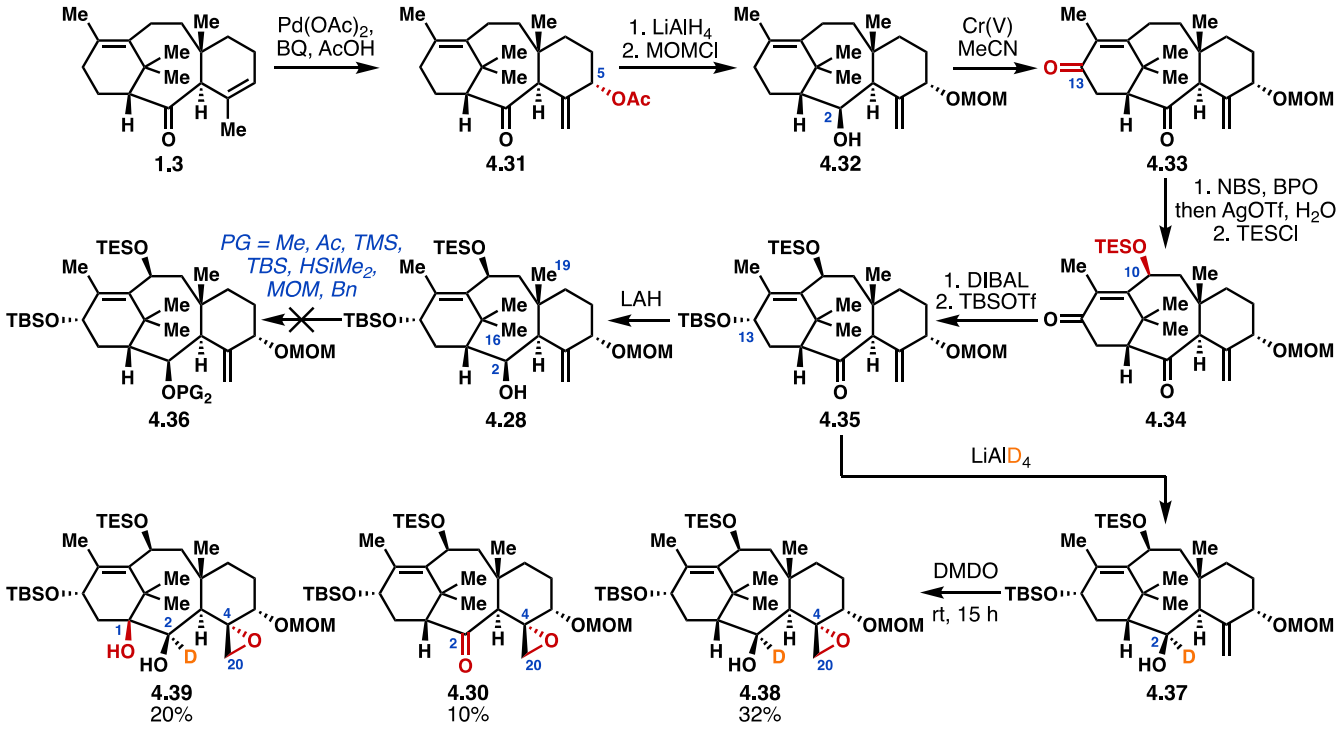

Figure 28. A second-generation oxidase phase designed for C1 oxidation.

substrates bearing various oxidation patterns and protecting groups were prepared (Figure 29b) in order to examine the C20 sterics, C20 directing effect, intramolecular protonation (from C1 and C20), intramolecular hydride delivery (from C1),[124] and B ring conformational effect (C10 α-OR and ketone substrates). The desired stereoisomer was never observed, and instead, either decomposition or C2 β-alcohol (as a single diastereomer) was observed. The decomposition was often observed for substrates bearing a C4 hydroxyl group (**4.43**), wherein a *retro*-aldol/aldol sequence could operate (Figure 29c). The possibility of such a pathway was shown by partial scrambling of the C4 hydroxyl stereochemistry when treated with base. The labile nature of this C4 alcohol significantly limits the scope of the reduction conditions and substrates. For example, a C4/20 epoxide opening was attempted but could not be achieved.

Thus, even though we managed to accomplish the much-desired C1 oxidation, the detrimental pitfall stemming from a vexing C2 reduction, forced us to abandon the route shown in Figure 28. In summary, this decision was taken because of four issues: (i) failure in stereoselective C2 reduction; (ii) unsuccessful C5 MOM deprotection (note that MOM groups survived DMDO), which was the reason oxetane-bearing compounds could not be prepared; (iii) no method to effect C7 oxidation; and (iv) poor material throughput.

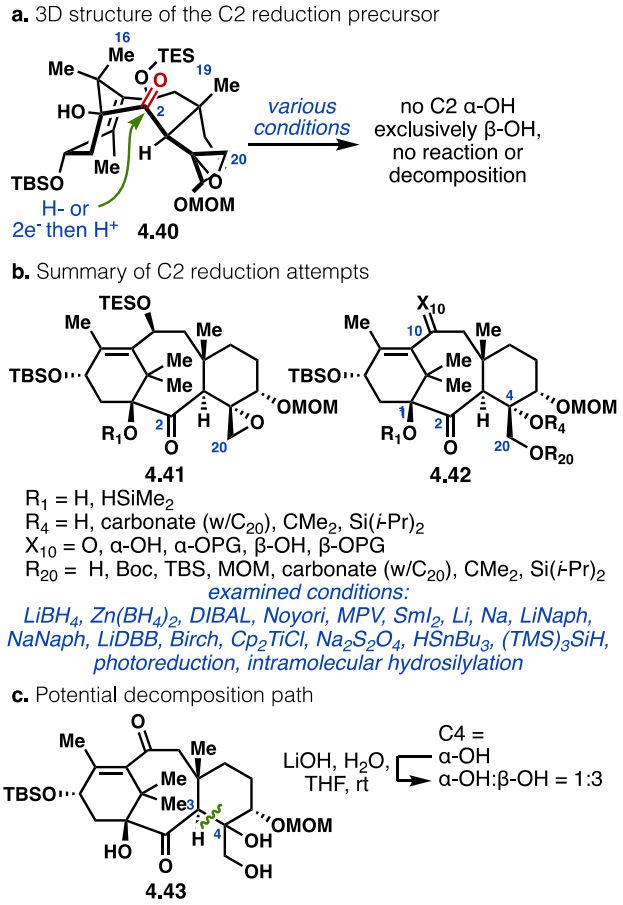

Figure 29. (a) 3D model-based illustration depicting the stereoselectivity of C2 reduction. (b) Representative attempts for C2 reduction. (c) Observed C4 epimerization.

5. An Oxidase Phase that Allows for C2 Stereoselective Reduction

5.1 C20 Desmethyl Oxidase Phase

The arduous challenges posed by C1 oxidation and C2 stereoselective reduction made us deeply reflect on literature precedent (Figure 30).[69,125–127] There are only four reported precedents of C2 α-stereoselective ketone reduction. Notably, an olefin isomer of **1.3** ($\Delta^{4,20}$ instead of the $\Delta^{5,6}$-olefin) exclusively gave the corresponding β-stereoisomer upon Bouveault–Blanc reduction.[69] These precedents suggested that the key for a successful C2 reduction was to create steric accessibility to C2, wherein space can be generated by avoiding a *pseudo*-equatorial substituent at C4, thus allowing more room for the C2 ketyl intermediate to adopt the α-configuration.

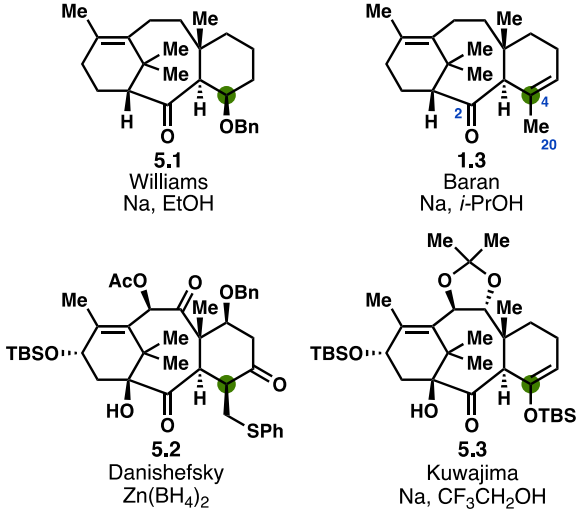

Figure 30. Literature precedent for α-selective C2 reduction.

Thus, requirements for a new oxidase phase entailed: (i) a route that avoids a C5 MOM group; (ii) a late-stage C2 ketone deuteride reduction; and (iii) minimization of steric hindrance at C4 to allow for C2 reduction. These conditions were met in the third-generation oxidase phase (Figure 31a). We thus started from a cyclase phase intermediate, C20 desmethyl taxadienone (**5.4**),[51] which allows access to substrates similar to **5.1**. By following a similar oxidation sequence to Figure 28, the pivotal DMDO oxidation precursor **5.5** was synthesized. To our dismay, this substrate underwent C4 benzyloxy to benzoate oxidation, followed by C2 oxidation, despite the presence of the α-deuterium. The C2 oxidation occurred too rapidly, perhaps because the removal of the C20 carbon made C2 too accessible for DMDO. Sterically and electronically deactivated substrates, C4 OTES (**5.7**) and C4 ketone (**5.8**), were equally unsuccessful and gave undesired products (Figure 31b). These outcomes indicated that the presence of a C5 substituent is necessary to affect the C ring conformation, such that the C4 functional groups can effectively protect C2 from DMDO while the C1 C–H still remains available for hydroxylation.

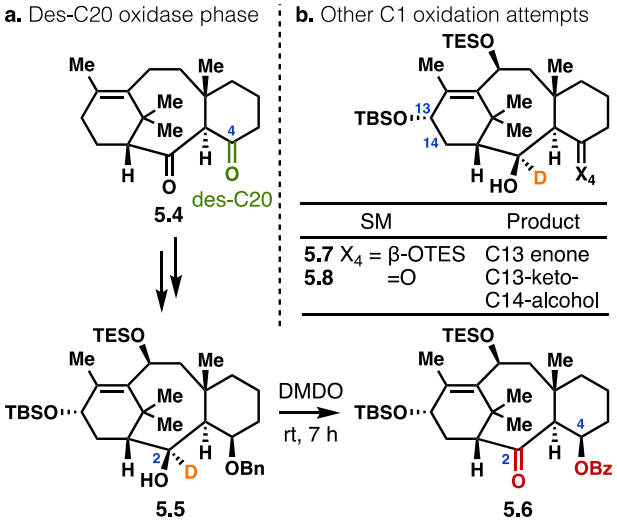

Figure 31. The third-generation oxidase phase. (a) C20 desmethyl oxidase phase. (b) C1 oxidation attempts with other substrates.

5.2 Studying a C2 Reduction Model

The abandoned third-generation route made it evident that meticulous substrate design (creating just enough steric hindrance around C2) was indispensable to realize both C1 oxidation and C2 stereoselective reduction. Thus, the next goal was to find a substrate that gives the desired C2 α-alcohol in the presence of a C20 carbon. Extensive substrate examination revealed that ketone **5.9** affords the desired diastereomer **5.10** in α:β = 2:1 ratio under modified Bouveault–Blanc conditions analogous to one employed in the taxabaccatin III (**1.5**) synthesis (Figure 32). The desired stereoselectivity likely arose from the C4 β-OH/α-Me substitution pattern, which could adopt a staggered conformation with the intermediate ketyl radical, and result in a thermodynamically more stable α-configuration. This C4 tetrasubstituted motif was also desirable to create a sufficient steric barrier around C2 that could direct DMDO onto the C1 C–H bond. This stereochemical outcome was not observed with other single-electron reductants (e.g., SmX_2),[128,129] which highlight the unique reactivity of this substrate and the reaction conditions.

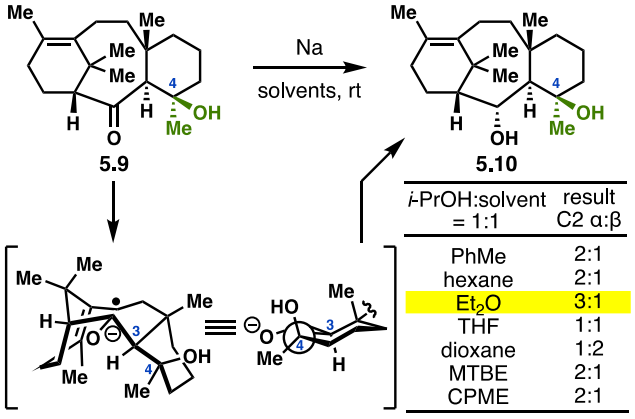

Figure 32. Success in the stereoselective C2 ketone reduction.

Further optimization showed that the PhMe-doped Bouveault–Blanc reduction conditions (Na, *i*-PrOH, PhMe) could drive the reaction to completion even at room temperature (previously conducted at 80 °C). Intriguingly, taxadienone (**1.3**) decomposed upon exposure to these conditions, which showcases the unique reactivity of **5.9**. Furthermore, reduction at lower temperatures slowed the reaction rate, and higher temperatures yielded a diverse set of impurities. Other proton sources such as MeOH, *t*-BuOH, TFE, thiols, and amines gave inferior reactivity, conversion, or stereoselectivity.[130] Reduction of PhMe was not observed even under Benkeser-type conditions,[131] where PhMe presumably serves as an electron mediator.[132] Other co-solvents exhibited a similar rate of acceleration as PhMe, even though the exact reaction mechanism might be different from the PhMe conditions. Ultimately, the best stereoselectivity was obtained when Et_2O was used as the co-solvent (giving α:β = 3:1 ratio). With the identification of a suitable C4 bearing tertiary alcohol substrate to effect stereoselective C2 reduction, we were hopeful that the precise oxidation pattern at C1 and C2 could be installed. This now left only one oxidation to install: the C7 alcohol.

6. Successful Oxidation of C7 by a Redox Relay Approach

6.1 Direct C7 Allylic Oxidation Attempts

Three unsuccessful oxidase phase routes were developed, but for each route, many roadblocks narrowed down the possible oxidation patterns. The structural requirements we had learned up to this point are summarized as follows (Figure 33): (i) a late-stage C2 deuteride reduction; (ii) a C4 tertiary β-hydroxyl group for α-selective C2 reduction (which would potentially guide the C1 oxidation event as well, by sterically protecting C2 from DMDO); (iii) installing a C5 substituent that would not necessitate a protecting group; and (iv) installing C10 and C13 bis(silyl)ether substituents to protect the bridgehead olefin from epoxidation. The stage was set to begin strategizing on how to introduce the C7 oxidation.

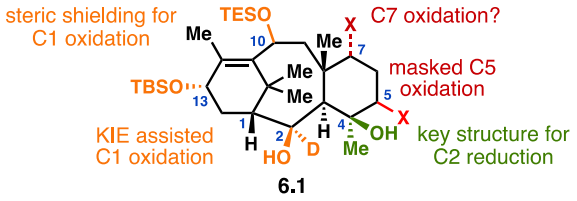

Figure 33. Requirements for the C1 oxidation and the subsequent, stereoselective C2 reduction.

C7 oxidation was never observed in the course of directed C–H oxidation attempts and TFDO/DMDO oxidations, which suggested that the C7 position requires some form of reactivity enhancement to undergo oxidation. First, compound **6.2** was synthesized because its oxidation pattern could be advantageous in downstream transformations (Figure 34): (i) the key C4 motif was already poised for the stereoselective C2 reduction; (ii) the $\Delta^{5,6}$-olefin serves as a C5 oxidation placeholder; and (iii) the functionalization of C6 would allow for a potential oxidation relay to C7. Compound **6.2** was tested against numerous allylic oxidation conditions, but C7 oxidation was never observed. Instead, oxidations at C11 (under ene and radical-based conditions) and C18 (with SeO_2 and CrO_3+DMP) were often observed, suggesting that the substrate's inherent reactivity at the bridgehead olefin is difficult to overcome. Therefore, the C13 position was oxidized first to suppress the $\Delta^{11,12}$-olefin reactivity (giving compound **6.3**). Unfortunately, C7 oxidation was not observed with this substrate either, despite the wide range of examined reaction modes, likely because of the sterically hindered nature of the target C–H bond.

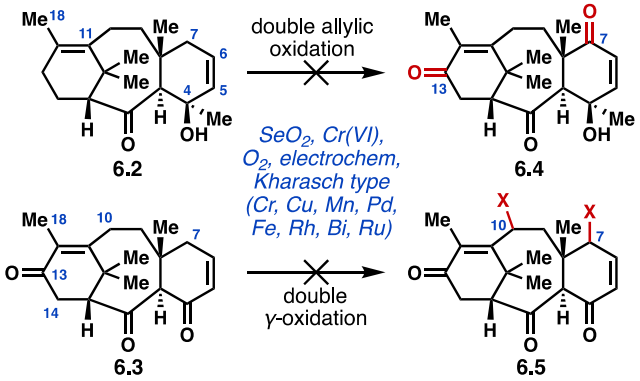

Figure 34. Allylic C–H oxidation attempts at C7.

6.2 Enolate-Mediated Saegusa-Type Oxidation

The poorly reactive C7 methylene indicated further activation is necessary to oxidatively functionalize C7. Dienone **6.6**, prepared from diketone **5.4** (see Figure 31) in 2 steps, was treated with TMSOTf to afford the thermodynamic vinylogous(silyl)enol ether at C13 at 0 °C, which further reacted to generate another vinylogous(silyl)enol ether at C4 (**6.7**) at room temperature (Figure 35). It is remarkable that such a strained molecule can be formed: 9 out of 14 peripheral carbons are *sp*² hybridized. This dramatic configurational shift completely altered the shape of this molecule from spheroid to L-shaped. This intermediate was treated with $Pd(OAc)_2$ to effect two Saegusa-type oxidations simultaneously, installing the oxidations at C7, C9 and C10 (thus giving **6.8**). The C7 acetoxy group was installed in an α-configuration (opposite to that of natural taxanes), caused by the L-shape of the precursor **6.7**.

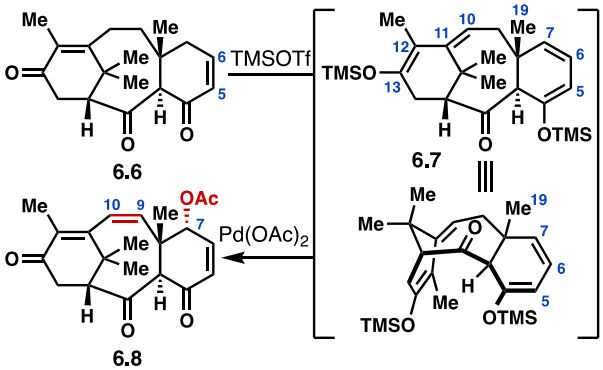

Figure 35. Saegusa-type double oxidation.

The proximity of the C7 methylene and the $\Delta^{9,10}$-olefin naturally lent itself to a directed oxidation strategy. The efficiency of the above transformation notwithstanding, compound **6.8** and its deacetoxylated form **6.9** could not afford any further oxidized products, and resulted in no reaction or decomposition under a variety of olefin oxidation conditions (Figure 36). While not surprising based on our prior findings (on triene **3.6** in Section 3.2), the hope was that the C7 oxygen could direct reactivity to this quasi-inert olefin. The C20 carbon was then installed with the hope of affecting the C ring conformation just enough to adjust the orientation of the C7 hydroxyl group (**6.10**). To our dismay, this maneuver did not change the outcome of the oxidant screening.

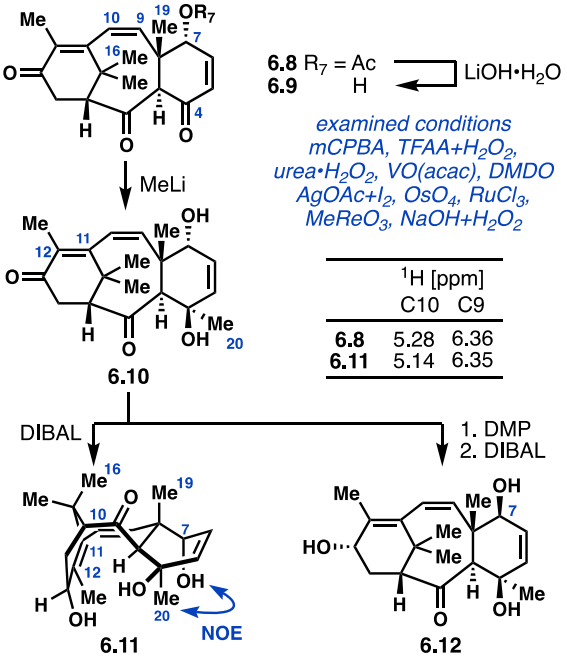

	^{1}H [ppm] C10	C9
6.8	5.28	6.36
6.11	5.14	6.35

Figure 36. C7 directed $\Delta^{9,10}$-olefin oxidation attempts.

We hypothesized that the poor reactivity of the $\Delta^{9,10}$-olefin in **6.8** might be caused by inductive and resonance deactivation from the C13 ketone. Indeed, the C9 and 10 ^{1}H NMR chemical shifts are relatively downfield (C9 and C10 protons: 6.36 and 5.28, respectively), while those of triene (**3.6**) exhibited more upfield shifts (C9 and C10 protons: 5.93 and 5.16, respectively).[65] Therefore, the C13 ketone was chemoselectively reduced with DIBAL to afford **6.11**. Contrary to our expectations, the C9 and C10 chemical shifts remained roughly the same, which means that the downfield effect was caused by neither induction nor resonance from the C13 ketone, but instead from an induced magnetic field from the bridgehead olefin. NOESY analysis of **6.11** revealed that the C ring adopts a boat conformation (NOE correlation between the C20 methyl and the C7 OH), which places the C7 alcohol at an appropriate configuration for the directed oxidation of $\Delta^{9,10}$-olefin from a relatively accessible concave face, opposite to the C16 and C19 methyl groups. However, **6.11** also did not undergo C9/10 oxidation. Furthermore, the C7 β-alcohol (**6.12**) was prepared, to inspect whether the C7 stereochemistry affects its directing ability. Unsurprisingly, the results were identical to those of **6.11**.

Unsuccessful outcomes from both C7 hydroxyl stereoisomers strongly suggested that, yet again, the $\Delta^{9,10}$-olefin was simply unreactive regardless of the presence of a directing group. Although this taxatriene approach ultimately allowed for the installation of a C7 β-alcohol, it represented a dead end as the C9/10 oxidations were no longer feasible.

6.3 Enolate-Mediated Double γ-Oxidation

We had learned from the bis(silyl)enol ether mediated double γ-oxidation strategy that the oxidation of C7 required high $\Delta^{5,6}$-olefin reactivity. Thus, the same compound **6.6** was treated with TMSOTf to generate the bis-vinylogous(silyl)enol ether *in situ*, however, this time, a Saegusa-type oxidation was not performed. Instead, electrophilic Cl, Br, or I was added, giving a C7 and C10 double-oxidation product **6.13** (Figure 37a). The C7 halogen was incorporated with α-configuration, as had been the case with Saegusa oxidation. To our surprise, the C10 halogen was also introduced with α-stereochemistry from the concave face, opposite to the β-configuration observed in the routes toward taxuyunannine D (**1.4**; see Figure 12) and taxabaccatin III (**1.5**; see Figure 20). Unexpectedly, S_N1-type C7 and C10 double solvolysis with AgOTf did not take place unlike with previous C10 β-Br substrates (Figure 37a inset table), presumably because the α-halides were confined in the concave face where the Ag atom could not approach. Instead, a triethylborane-mediated radical dehalogenation[133] successfully replaced both iodides with hydroxyl groups, although it proceeded in a stereoretentive fashion at both C7 and C10.

This C7α and C10α bis-hydroxyl compound could be prepared in a more direct manner by treating the bis-vinylogous(silyl)enol ether with $^1O_2$. The bridged peroxide **6.15** was stable enough to be isolated by preparative TLC, but was not stable under basic conditions, and treatment with triethylamine led to decomposition. Perplexingly, the C10 hydroperoxide was never observed. In the end, DMS was used to reduce the endoperoxide and afford **6.16**, which could be selectively TES-protected at C10 to give **6.17**. After C4 methylation to give **6.18**, the stage needed to be set for the C1 oxidation: this setup sequence included C13 reduction, C13 protection, C7 protection and C2 reduction. A C7 oxidation and C7 reduction sequence could also be performed if the C7 stereochemistry needed to be corrected to β at this stage (direct stereoinversion via Mitsunobu conditions, the Tsunoda reagent[134–136] and rhenium catalysis[137,138] were not effective). After testing every possible permutation of the above transformations, it became critically clear that there was no selective way to realize them. The protections at C7 and C13 were particularly problematic not only in the sense of selectivity, but also compatibility: we could not devise a protecting group that is orthogonal to silicon-based protecting groups (C10 TES is as labile as TMS), and survive harsh conditions (DIBAL, $LiAlD_4$, DMDO, Na) until the very end of the synthesis. Despite a series of poor selectivities and low yields, small quantities of the desired product were carried forward to arrive at **6.19** since our primary interest lied in the C1 oxidation and C2 reduction. However, to our great disappointment, DMDO oxidized

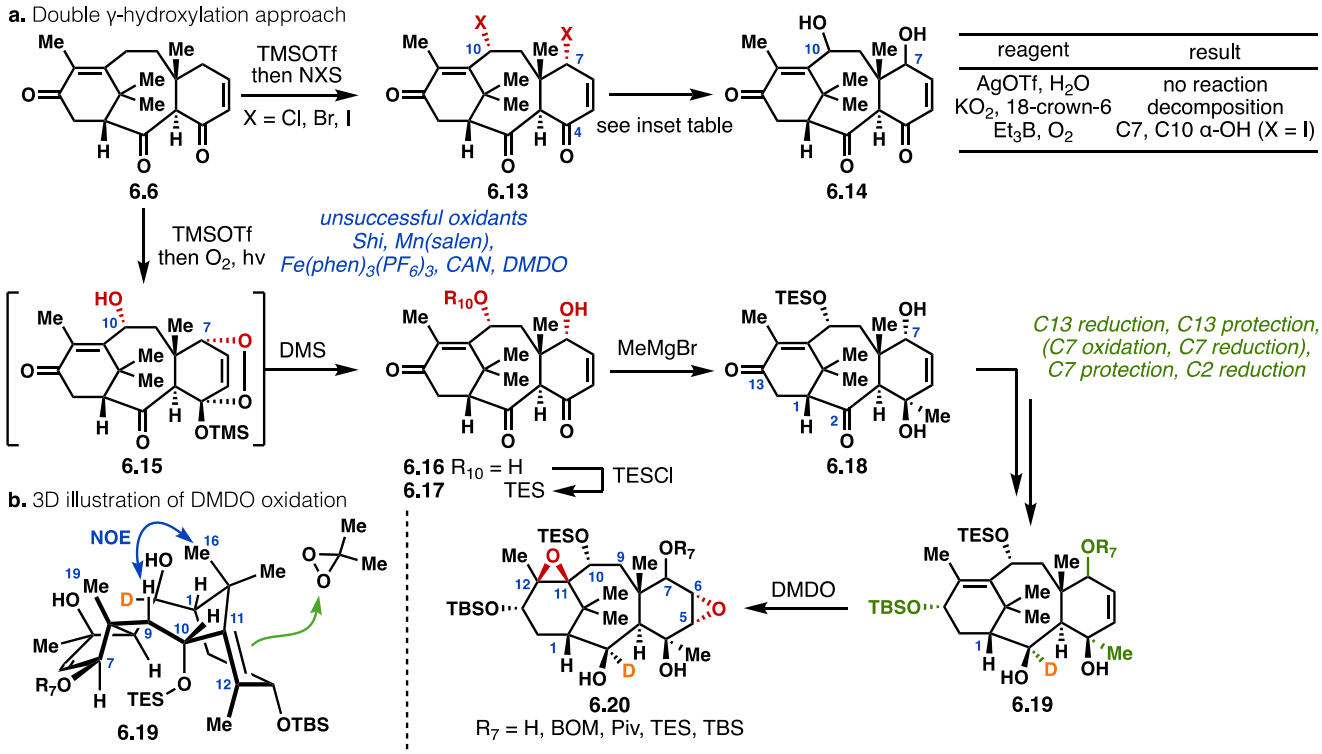

Figure 37. The fourth-generation oxidase phase. (a) Steps toward a DMDO precursor via a bis-vinylogous(silyl)enol double γ-hydroxylation route. (b) A 3D representation of **6.19** that accounts for oxidation regioselectivity.

the $\Delta^{5,6}$- and $\Delta^{11,12}$-olefins to give **6.20**, and C1 oxidation was not observed. The bridgehead olefin epoxidation seemed to retard the C1 C–H reactivity. This unexpected chemoselectivity was tracked by careful NOESY analysis, which revealed that the C10 α-OTES group adopted an axial conformation despite its steric bulk, and that the B ring correspondingly resided in a twist-boat conformation (Figure 37b). This conformation is probably energetically more favored than the other possible conformer, boat-boat, by circumventing steric clashing between the C2 β-alcohol, and C16 and C19 methyl groups, which is probably more significant than the steric penalty caused by an axial OTES group. The conformation of the C10 α-OTES rendered the $\Delta^{11,12}$-olefin more exposed, and therefore allowed facile epoxidation by DMDO. The outcome of DMDO oxidation was more or less the same regardless of the C7 stereochemistry, and regardless of the presence of a C7 protecting group: the desired C1 oxidation product was simply not observed.

With these unsatisfactory results, this fourth-generation oxidase phase route had to be abandoned due to the following insurmountable problems: (i) poor material throughput (C13 allylic oxidation in 30% yield, poor selectivity for C20 methyl installation, non-selective C7 protection); (ii) no suitable protecting groups for C7; (iii) the undesired C7 stereochemistry; and, most critically, (iv) unsuccessful C1 oxidation. However, there were two major learnings through this oxidase phase: (i) it became clear that a C10 β-OTES group was effectively protecting the bridgehead olefin from DMDO (see Figure 28); and (ii) installation of the C7 alcohol is possible from a $\Delta^{5,6}$-olefin by redox relay through a bis-vinylogous(silyl)enol ether. However, at this point, we hypothesized that the choreography of C7 oxidation was incorrect. It is worth reiterating that one of the most challenging aspects of a Taxol® (**1.1**) synthesis is that there are too many similar functional groups, which inflict minute conformational changes caused by a relatively flexible B ring. Comprehending the subtle changes and differences of each secondary alcohol is therefore essential for the completion of **1.1**. We viewed this as an opportunity to do a deep dive into oxidation choreography: Which oxidation state should be introduced in what form, in what order, and at what stage of the synthesis to maximize the divergency and feasibility of the entire synthesis? This was the fundamental question that we sought to answer as we entered the fifth and final generation of the oxidase phase.

7. Two-Phase Synthesis of Taxol®

7.1 Rational Design of the Final Oxidation Choreography

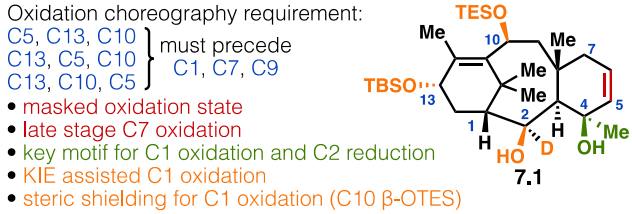

Figure 38. All clues lead to taxane intermediate **7.1** as a candidate from which to commence the final oxidation choreography.

The four abandoned routes discussed so far contained a treasure trove of clues that guided the journey through the

oxidase-phase maze posed by Taxol® (**1.1**). These clues, taken together, provided a number of essential insights regarding structure–reactivity relationship of the taxane skeleton. This led to the proposal of a taxane skeleton that would be most likely to lead to **1.1**: taxane **7.1** (Figure 38).

First, masked alcohols (or synthetic equivalents thereof) on C5, C10 and C13 needed to be installed before the C1 oxidation. A functional group on C5 seemed to be required to properly set the C ring conformation and induce C1 oxidation (compare the second- and third-generation oxidase phases in Figure 28 and 31, respectively). Since C5 oxidation had to take place at an early stage, incorporating it as an inert alternative would be more strategic to avoid potential protecting group issues. The fourth-generation route demonstrated that early-stage introduction of any hydroxyl group that is not critical for reactivity of other parts of the molecule imposed an extra burden on Taxol's ever-challenging chemoselectivity puzzle (Section 6.3). From a reactivity perspective, neither directed (Section 4.1) nor allylic C7 oxidation (Section 6.1) was conceivable, which compelled us to conduct an oxidation relay from C5 to C7. Thus, a $\Delta^{5,6}$-olefin was deemed to be a suitable oxidation state placeholder.

C10 and C13 substituents that sterically protect the $\Delta^{11,12}$-olefin from DMDO were also essential groups to be incorporated prior to DMDO oxidation of C1. The developed C10 oxidation method necessitates the presence of a C13 enone (Section 2.4); therefore, the C13 oxidation should take place prior to C10 oxidation. Paradoxically, the protecting group on C13 has to remain stable until the very end of the synthesis (before the side chain attachment), but the deprotection conditions must be mild enough for high functional group tolerance. One of the most reliable protecting groups that meets these criteria is TBS.[18,23] Furthermore, the C10 substituent needed to be formed with β-stereochemistry to be an effective protecting group for the bridgehead olefin (Section 6.3). The C10 alcohol protecting group must also survive a number of harsh reaction conditions and be distinguishable from the C13 OTBS. Therefore, TES was selected for that position.

The C2 α-deuterium is an essential non-canonical protecting group to kinetically suppress the competitive C2 ketone formation during the C1 oxidation. The C4 β-*tert*-alcohol is the critical element that enables C1 oxidation and C2 stereoselective reduction. This hypothesis hinged on the observation that neither an epoxide nor a diol allowed C2 reduction, and a *tert*-alcohol was the sole remaining functional group that could be easily derivatized to a diol (via dehydration/dihydroxylation) for oxetane closure.

7.2 Oxidation Choreography of C5, C10, and C13

As the fourth-generation oxidase phase suggested, the C20 desmethyl taxane (**5.4**) was chosen as a starting point to accomplish both the installation of the critical C4 β-OH α-Me moiety as well as a potential oxidation relay to C7. As depicted in Figure 38, there are three different oxidation choreographies to arrive at **7.1**. It was empirically discovered that C10 oxidation was extremely dependent on the C5 functional group (Figure 39 inset table), and this determined the early-stage oxidation choreography. This slight structural modification substantially affected the reactivity at the other side of the molecule as a consequence of the conformationally flexible medium-sized ring. However, it is worth mentioning that the two-phase approach was advantageous to rapidly examine all the possible order of operations since the carbon skeleton (with the exception of C20) was already fully assembled, while a traditional convergent approach would have necessitated a new synthetic route to each substrate.

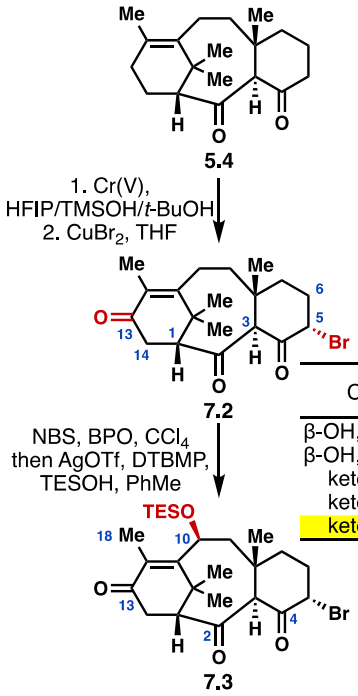

Solvent	Yield [%]
$PhCF_3$	trace
MeCN	20
HFIP	trace
TMSOH	trace
HFIP, TMSOH	50

C4	SM (C5,C6)	Product C10:C18
β-OH, α-Me	olefin	1:1
β-OH, α-Me	CH_2, CH_2	trace
ketone	olefin	1:1
ketone	CH_2, CH_2	1:1
ketone	Br, CH_2	1:0

Figure 39. The final oxidation sequence for C5, C10 and C13. DTBMP, 2,6-di-*tert*-butyl-4-methylpyridine.

The above considerations led to an extensive optimization of the C13 allylic oxidation on **5.4** (originally achieved in ca. 20% yield in MeCN) to improve the material throughput, considering that this was the very first reaction of the oxidase phase (Figure 39). As mentioned previously (Section 2.3), Cr(V) is a unique reagent that regioselectively oxidizes the C13 position without oxidative cleavage of the $\Delta^{11,12}$-olefin. Although the paramagnetism of Cr(V) limited mechanistic studies by NMR and the limited literature information on such complexes rendered optimization challenging, the oxidation is reported to be highly solvent dependent ($PhCF_3$, MTBE, MeCN).[68,69,88] Solvent screening unearthed the finding of a curious solvent combination, HFIP and TMSOH (pK_a = 11),[139] as the optimal solvent system for this transformation. This yield enhancement was only observed when both HFIP and TMSOH were used, however, this synergistic effect remains mechanistically unclear. Ultimately, a ternary solvent mixture was employed on scale by addition of *t*-BuOH, which was found to play a crucial role in solubilizing the Cr(V) reagent.

Our studies in oxidation choreography revealed that C5 should be the next carbon to be oxidized. However, as with C7, installation of a hydroxyl group would cause protecting group manipulation issues downstream, and therefore the oxidation had to be: (i) tolerant to NBS (used for C10 oxidation); (ii) readily transformable to a $\Delta^{5,6}$-olefin for the future oxidation relay to C7; and (iii) readily installable. These requirements led us to use a bromide as an oxidation state placeholder. To this end, $CuBr_2$ was employed as a mild α-bromination reagent and, delightfully, gave C5 bromide **7.2**. The cleanest reaction profile was obtained in THF, furnishing **7.2** in 55% yield over two steps (C13 then C5 oxidation). The remarkably site-selective α-bromination of the C4 ketone was attained by taking advantage of the innate reactivity of the taxane skeleton. C1 and C3 are virtually non-enolizable, and enolate formation at C14 would form a strained bridgehead diene, which left only the C5 position as the readily enolizable position. The installation of three ketones in this compact scaffold might look non-strategic, however, this maneuver was made with the confidence that their reactivities are vastly different.

The subsequent C10 oxidation from **7.2** to **7.3** proceeded without C5 debromination or radical fragmentation. The uniquely high site selectivity at C10 was significantly influenced by the C5 substituent, which was one of the reasons why C5 was oxidized not by Saegusa oxidation, but by bromination (Figure 39 inset table). A potential explanation for this dramatic change in selectivity is that the C5 bromine might force the C ring to adopt a boat conformation upon heating, which affects the B ring conformation as well, permitting the C10 C–H antibonding orbital to have a better orbital overlap with the bridgehead olefin. The subsequent solvolysis with TESOH regioselectively proceeded at C10 because the C5 position is adjacent to a ketone, where carbocation formation is unfavored.

7.3 C1 C–H Oxidation with DMDO

The reactivity difference of the carbonyl groups at C2, C4 and C13 in **7.3** was fully exploited to arrive, without additional detours, at the key C1 oxidation precursor **7.1**. To our delight, a solution of DMDO in acetone oxidized **7.1** to afford **7.4** in appreciable yield, along with **7.5** and **7.6** (Figure 40). A reactivity comparison between C2 deuterium- and hydrogen-containing substrates validated the presence of a KIE (Figure 40 inset table). However, this reaction in acetone could not be pushed to completion (thus leading to large amounts of incomplete oxidation product **7.5**), since extended reaction times resulted in another side product: a C13 enone (not shown). Additives, co-solvents and numerous other reaction variables were examined,[140] however, the reaction yield did not improve. Although the efficiency of dioxirane-mediated C–H oxidation is remarkably dependent on its concentration,[38] inconveniently, the concentration of DMDO in acetone cannot exceed 0.1 M, or it will undergo Baeyer-Villiger oxidation with the solvent. Therefore, extracting DMDO into an oxidation-resistant solvent and washing away the acetone would allow for the preparation of a more concentrated DMDO solution. Messeguer studied the extraction efficiency of DMDO with various oxidation-resistant solvents, and quantified how the acetone content in the extracts varied for each solvent as well as for the number of washes.[141] As such, using a higher concentration of DMDO to oxidize **7.1** improved the product distribution (Figure 40 inset table), which significantly decreased the labor associated with substrate recycling, and increased the overall material throughput. $CHCl_3$ was a particularly effective solvent, presumably because it enhances the reactivity of DMDO through H-bonding.[140] Non-polar solvents such as CCl_4 and $PhCF_3$ led to uncharacterized decomposition, while Na_2SO_4-dried DMDO solution in $CHCl_3$ completely degraded the substrate. Trace amounts of water were beneficial to suppress DMDO's activity just enough to oxidize the C1 C–H bond, and simultaneously protect the substrate from oxidative decomposition.

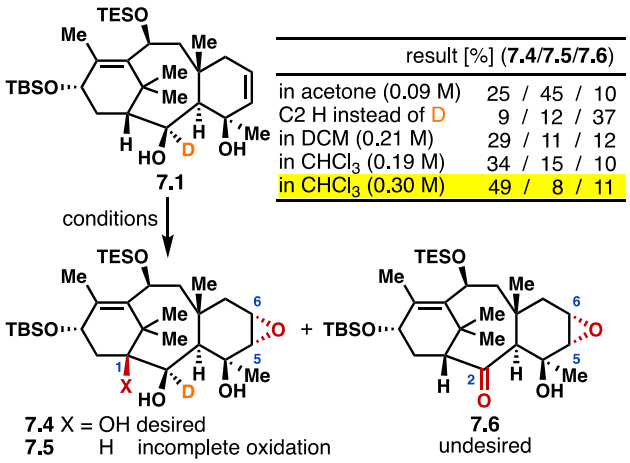

Figure 40. Optimization of the C1 oxidation.

This successful outcome indicated that our substrate design for **7.1** was finally correct with all the following points fully leveraged; (i) the $\Delta^{11,12}$-olefin protection using the C10 β-OTES and C13 OTBS groups (Sections 4.3 and 6.3); (ii) the C2 β-stereochemistry, which removed enough steric hindrance for DMDO to approach the C1 C–H bond (Section 4.4); (iii) the C2 α-deuterium atom, which served as the smallest "protecting group" that kinetically guided the C1 oxidation (Section 4.3); and (iv) the C4 tetrasubstituted carbon, which also protected C2 from competitive oxidation (Section 5.1).

7.4 Substrate Guided C2 Reduction

Although the C1 oxidation was now feasible in moderate yields, this route would not be successful without stereoselective C2 reduction. To this end, Ley-Griffith oxidation of C2 removed the deuterium and afforded keto alcohol **7.7** (Figure 41), which contains the C4 *tert*-β-hydroxyl group that was essential for the stereoselective C2 reduction (Section 5.2). Bouveault-Blanc reduction conditions that were optimized earlier worked with good stereoselectivity to furnish **7.9** with the C5/6 epoxide completely unscathed. As discussed in Section 5.2, it is possible that the C4 substituents allowed a staggered conformation with the C2 alkoxide in ketyl intermediate **7.8**, which generated a persistent α-conformer, leading to **7.9**.

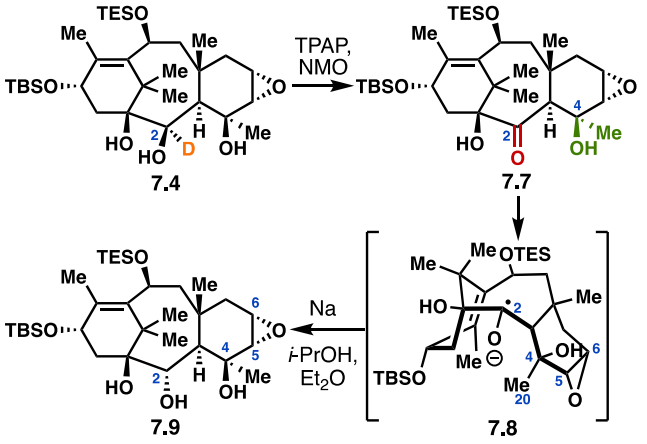

Figure 41. Establishing the C2 α-alcohol.

7.5 C7 Redox-Relay

With the C5/6 epoxide **7.9** in hand, a redox-relay strategy[46,47] emerged as the best tactic to achieve the C7 oxygenation (Figure 42). After protecting the C1 and C2 alcohols of **7.9** as the carbonate to give **7.10**, Lewis acid screening revealed that BF_3•OEt_2 with TBAI at cryogenic temperatures could drive the iodohydrin formation to completion. However, this product **7.11** was unstable, and reverted to **7.10** during purification, resulting in inconsistent yields. One-pot addition of TMSIm led to C5 alcohol protection, but also to an undesired C10 protecting group swap from TES to TMS (compound **7.13**). The addition of typical Lewis bases (e.g. pyridine and Et_3N) reversed the reaction to give the starting **7.10**. Investigation of sterically or electronically biased pyridine derivatives revealed that 2-fluoropyridine can act as a mildly basic boron quencher, allowing for selective formation of **7.12** with the addition of TMSIm to **7.11**.

Treatment of compound **7.12** with DMDO immediately formed iodoso species **7.14**, which underwent spontaneous regioselective *syn*-elimination to liberate olefin **7.15**. This outcome was consistent with unsuccessful base-induced E2 elimination attempts from **7.11** to **7.15**. Notably, this iodoso group was such a potent leaving group that a competitive epoxide reclosure path, where the OTMS group attacks the C6 carbon to regenerate **7.10**, was operative. Unfortunately, this reaction suffered from reproducibility and scalability challenges. In search of a more robust oxidation protocol, metal-mediated iodide oxidations were explored. Successful iodide oxidation with $Mo(CO)_6$,[142] Li_2MoO_4, Ag_2MoO_4 and $W(CO)_6$[143,144] in combination with TBHP could in fact be achieved. The oxidation did not proceed with Fe and V or only with TBHP, suggesting the involvement of an *in situ* generated molybdenum- and tungsten-peroxo species. Disappointingly, these conditions normally stalled at olefin **7.15**, while DMDO could oxidize the resulting olefin to the epoxide.[145] Even though a small amount of epoxide **7.16** was observed with $Mo(CO)_6$-mediated conditions, the steric hindrance around the $\Delta^{6,7}$-olefin rendered the epoxidation very sluggish. Ultimately, exposure of **7.12** to excess DMDO in acetone in the presence of phosphate buffer solved the reproducibility issues and cleanly effected iodoso elimination and tandem $\Delta^{6,7}$-olefin epoxidation to afford epoxy-taxane **7.16**. This entire maneuver (**7.10** to **7.16**) was achieved without isolation of unstable intermediates through a precisely elaborated sequence involving the addition of orthogonally reactive and volatile reagents.

Finally, the oxidation relay was completed by regioselective reduction. The high functional group tolerance (C1/2 carbonate, C4 *tert*-alcohol, C5 OTMS, C10 OTES) of the Nugent-RajanBabu reagent[146–148] is widely appreciated in the total synthesis of complex molecules.[149] Addition of an organosilane dramatically improved the mass balance presumably via facile quenching of the C6 radical resulting from the epoxide opening, while common additives such as water and collidine retarded relayed from the C4 ketone to C5 bromide, $\Delta^{5,6}$-olefin, C5/6 epoxide, C6 iodide, $\Delta^{6,7}$-olefin, C6/7 epoxide, and finally to the C7 alcohol. Each functional group served as an oxidation state placeholder that, at least in this context, did not require protecting groups, and played a substantial role in setting the stage for remotely guiding other transformations (C10 bromination, C1 oxidation, and C2 stereoselective reduction).

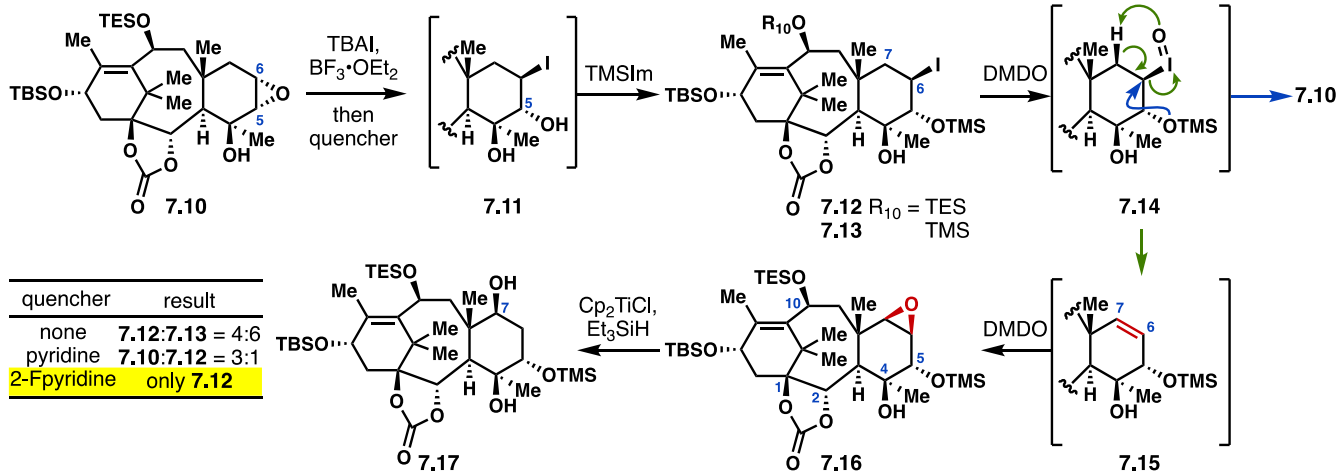

Figure 42. The C7 oxidation relay sequence.

7.6 Completion of the Synthesis

Armed with all the knowledge of oxidation tactics, choreography and optimized conditions, the two-phase synthesis was carried out as shown in Figure 43. The early-stage oxygenation (C5, C10 and C13) sequence started with the Cr(V)-mediated regioselective C13 oxidation, which introduced a functional group indispensable to taxane bioactivity at the first step. Subsequent C5 bromination proceeded with perfect regioselectivity, and then the previously developed C10 oxidation furnished **7.3**. Although in a different order compared to taxabaccatin III (**1.5**),[69] the same carbons were still oxidized in the early stages. When using C20 desmethyl taxane **5.4** as the starting material, the best regioselectivity was achieved.

The middle-stage oxidations required some oxidation choreography reevaluation to enable the key C1 oxidation and C2 stereoselective reduction. The C7 oxidation relay was placed after the pivotal C1 oxidation due to compatibility issues with the required functional group manipulations (i.e., $LiAlD_4$, DMDO, and Na). This sequence was completed with the regioselective C6/7 epoxide reductive opening from compound **7.16** to give **7.18**.

With most of the difficult challenges addressed earlier, transforming taxane **7.18** into Taxol® (**1.1**) was relatively straightforward in terms of oxidations, relying on literature precedent, and on a carefully planned oxidative end-game. The C4/20 position was oxidized at the late stages (**7.20**) much like in biosynthesis, although C9 oxidation became our last oxidation (**7.22**) while biosynthesis oxidizes C9 in the middle stages. Because of this decision to install C9 oxidation last, this route benefited from Holton's late-stage keto-alcohol tautomerization to furnish **7.23**, which only needed 2 more steps to complete Taxol® (**1.1**).[18] The final side chain installation was completed with benzyl-protected β-lactam **7.24**, which had never been utilized in the context of taxane total synthesis,[150] to enable a tandem one-pot deprotection of the benzyl group and C7 BOM group.

Overall, the difference in oxidation choreography from the original biomimetic plan to that of the final synthetic route to Taxol® (**1.1**) is of note. The early-stage oxidation choreography remained almost identical across the two-

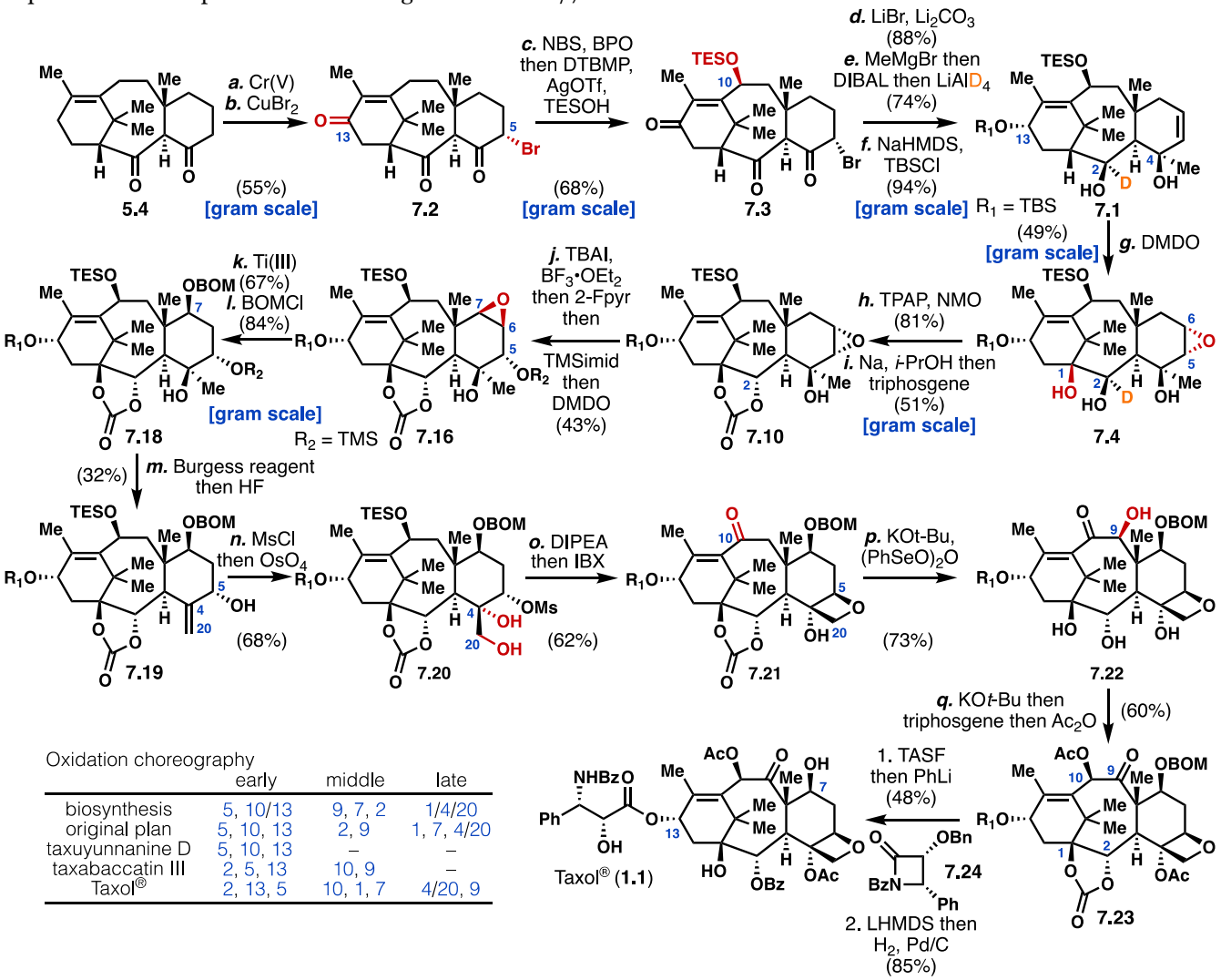

Oxidation choreography

	early	middle	late
biosynthesis	5, 10/13	9, 7, 2	1/4/20
original plan	5, 10, 13	2, 9	1, 7, 4/20
taxuyunnanine D	5, 10, 13	–	–
taxabaccatin III	2, 5, 13	10, 9	–
Taxol®	2, 13, 5	10, 1, 7	4/20, 9

Figure 43. Fifth and final generation of the two-phase synthesis of Taxol® (**1.1**).

phase syntheses of the three taxane targets, **1.4**, **1.5** and **1.1**. On the other hand, the middle- and late-stage oxidations required more functional-group-dependent planning, which established the sequence of C1, C2 and C7 oxidations. However, our primary goal of maximizing a potential analog output was still fulfilled by the early-stage installation of the C2 and C13 oxidation states, which are critical to taxane bioactivity.[151] As such, all intermediates including and beyond **7.1** meet the minimum structural requirements to enable medicinal chemistry explorations on the taxane framework.

8. Summary

8.1 Evaluation of Tactics

Our 13-year synthetic journey to Taxol® (**1.1**) entails both the cyclase phase[51] and the oxidase phase,[67–69] adhering to most of the guidelines originally laid out in our strategy, i.e., two-phase synthesis logic.[54] However, in order to achieve the synthesis of progressively complex and oxidized compounds taxuyunnanine D (**1.4**), taxabaccatin III (**1.5**) and Taxol® (**1.1**), deeper considerations of functional group interplay (oxidation choreography) were required, which resulted in several rounds of route revision.

For the first target, taxuyunnanine D (**1.4**), laboratory findings correlated well with the biosynthetic choreography, wherein chemoselective oxidants for each allylic position (C5, then C13 and C10) of taxadiene (**1.2**) were discovered (see Figure 12). This proof-of-concept in the two-phase taxane synthesis paved the way toward a taxane at a higher oxidation level. For taxabaccatin III (**1.5**), which bears additional oxidation at C2 and C9, taxadienone (**1.3**) was used as the starting point (and thus circumventing the need for C2 oxidation), with the C9 oxidation being carried out at the end. The synthesis from taxadienone (**1.3**) to taxabaccatin III (**1.5**) might appear to have proceeded as planned, however, it was not without hurdles, and orthogonal synthesis routes were also envisioned.[65,69] Strategic decisions on oxidation choreography were essential to install all the oxygenated functional groups at the proper oxidation level. Tactical learnings and adjustments in the synthesis of taxabaccatin III (**1.5**) include (see Figure 20): (a) C13 must be a ketone for the C10 oxidation, but it must be a protected alcohol during the C9 oxidation; (b) the C2 ketone of taxadienone (**1.3**) must be reduced and protected for C9 oxidation, and thus the C2 and C9 reductions cannot be performed simultaneously; (c) despite the known precedent for C9 α-oxidation,[18,20,26] this transformation encountered tremendous challenges in the synthesis of taxabaccatin III (**1.5**) as opposed to that of Taxol® (**1.1**). This observation was consistent with the unpredictable nature of the taxane skeleton due to the medium-sized ring: every functional group on the taxane framework could affect the reactivity of another position, regardless of the apparent proximity. These subtle changes in stereoelectronic, and more importantly, conformational effects, were found to present numerous challenges in the synthesis of **1.1**.

The milestones of taxuyunnanine D (**1.4**) and taxabaccatin III (**1.5**) syntheses paved a tactical foundation in our quest to access Taxol® (**1.1**). The allylic oxidation choreography laid at the outset of **1.4** was directly applied for the synthesis of **1.5**. It necessitated slight revision for the synthesis of **1.1**, because, to enable both C1 oxidation and C2 reduction, diketone **5.4**, which is a desmethylated version of the taxane skeleton, had to be used as the starting point. Even though this forced a slight deviation from the cyclase-then-oxidase strategy, since the C5, C10 and C13 atoms are also present in the desmethyl taxane skeleton, the robustness of the tactics still held. The two remaining C–H bonds on C1 and C7 could not be functionalized with our original plans of directed oxidation from neighboring carbon atoms (C2 and C9). The intermediates from the synthesis of taxabaccatin III (**1.5**) were used in our assessment of various oxidase phase routes toward Taxol® (**1.1**), and the route to **1.5** gave us a glimpse of how taxane's unique stereoelectronic and conformational effects render oxidation reactions highly dependent on substrate control. This further expanded our understanding of the oxidation choreography and guided us to strategic route scouting. The introduction of the C1 oxygen atom was ultimately performed using DMDO, which necessitated a deuterium-assisted non-canonical C2 protection as well as a stereochemically and conformationally based substrate design at C2 and C4. This obligated a late-stage thermodynamic C2 reduction unlike the taxabaccatin III (**1.5**) synthesis, thus leading to several rounds of new route scouting. The final C7 functionality had to be installed by a stepwise oxidation relay sequence. On a positive note, this avoided the use of conventional protecting groups within this context, which would have caused compatibility issues with other reaction conditions along the route.

8.2 Evaluation of Strategy

For the milestone targets of taxuyunnanine D (**1.4**) and taxabaccatin III (**1.5**), two-phase synthesis logic appears to be a favorable approach, generating these taxanes efficiently in 12 and 19 steps, respectively. The respective cyclase phase endpoints of taxadiene (**1.2**) and taxadienone (**1.3**) are good entries into the oxidase phase, minimizing redox and functional group manipulations. Both syntheses provided satisfactory answers to the original hypothesis that such a two-phase route would be both divergent and efficient. However, assessing whether Taxol® (**1.1**) was a suitable platform to test its utility depends on the point of view. On the one hand, the number of transformations required to reach **1.1** is less compared to previous total syntheses, and although a larger amount of **1.1** has been synthesized in this total synthesis campaign over others, it required a great amount of reaction and experiment choreography with a low overall yield. The route also represents a reasonable blueprint with which one could base a medicinal chemistry exploration if semi-synthesis were not possible. Such a strategy was utilized on ingenol to decipher unique bioactivity and selectivity as a function of precise oxidation pattern.[36] On the other hand, the proximity of functional groups on the taxane skeleton, and the

conformational flexibility requiring route redesign were challenges exacerbated by the inherent linear nature of the two-phase logic. The density of functional groups could perhaps be forged better by a convergent synthesis, and the conformational unpredictability of the taxane skeleton as well as protecting group manipulations would be less problematic if the full carbon skeleton is forged at the very end. Such an approach, however, would likely not be ideal for medicinal explorations.

Even at the outset of the two-phase terpene total synthesis program in 2009,[33,34] it was clear that advancements in C–C bond forming methodology were powerful enough to access minimally oxidized terpene scaffolds in short order. As clearly pointed out then, it is in the oxidase phase where synthetic chemistry has great opportunity for advancement.[54] This prediction was certainly borne out in the Taxol story as the taxane core could be easily made on scale in a handful of steps and the true challenge resided in the oxidase phase. Thus, two tactics that could dramatically improve our ability to mimic the oxidase phase include improved reactivity prediction methods and chemoselective oxidation reactions. The synthetic chemistry community has already begun addressing these challenges: a computational approach to predict the conformation and reactivity of complex substrates,[152] and chemoenzymatic reaction development for highly chemo- and regio-specific oxidations.[153] Despite current substrate limitations, these fields are dramatically advancing and will be widely in use by more and more synthetic chemists in the decades to come. At the same time, further chemical methodology development is still needed for the community to satisfy the demand for exquisite selective late-stage oxidations.[154–156] With such tactics in hand, medicinal chemistry-oriented complex terpene synthesis could be further simplified and become more widespread in the future.

8.3 Concluding Remarks

Taxol® (**1.1**) is an iconic terpene that is arguably the most demanding context to explore two-phase synthesis logic. Most previous syntheses had the specific purpose of probing whether a total synthesis of **1.1** was possible in the early 1990s, as well as understanding the chemistry surrounding **1.1**. Considering that neither objective is of much value today, how can the lessons obtained in this synthetic campaign be useful?

One of the reasons why two-phase logic has been demonstrated to be powerful is because it can forge the entire skeleton and maximize access to bioactive structures by mimicking biosynthesis. Considering that Taxol® (**1.1**) and other taxanes are bioactive, it is possible that intermediates that are created in the laboratory *en route* to **1.1** or other custom-designed taxanes with a certain oxidation pattern might display some bioactivity as well. Although the utility of natural products for drug discovery has stirred much debate,[157] it is undeniable that natural products have historically been the source of inspiration for countless medicines, whether they be analgesic, antibacterial, antifungal or anticancer agents. If renewed interest in the medicinal chemistry of the taxane family were to occur, one would need to systematically assess the effect of each oxygen atom in the taxane pharmacophore. Although previous reports of structure-activity relationships in this family relied on deconstruction/deoxygenation of Taxol® (**1.1**),[158] this current campaign provides synthetic accessibility to both lowly (which has yet to be investigated) and highly oxidized taxanes in a bottom-up manner.

Some of the choices we have made in the oxidative ascent of the taxane pyramid were guided by the number of natural taxanes displaying a certain oxidation pattern, and by the role of specific locations of the molecule regarding bioactivity. For example, C2 was chosen as the first oxygenation (i.e., for the cyclase phase endpoint, taxadienone (**1.3**)), not only due to the retrosynthetic simplification, but also because of its prevalence in natural taxanes, and its critical role in bioactivity.[159] Also, structure-activity studies on **1.1** have identified the side chain on the C13 oxygen atom as one of the requirements for biological activity.[158,159] Thus, the oxidation at C13 was chosen as our second site of oxidation. Accessing C5 oxidation is also important (which is oxidized thereafter),[160] and while elaboration of C5/20 to the oxetane is deemed critical, the synthesis of the oxetane could be achieved earlier in the synthesis if it were not for the C7 oxidation. Interestingly, 7-deoxytaxol is as cytotoxic as Taxol® (**1.1**),[161–163] and therefore C7 oxidation is seemingly unnecessary, which would render a purely synthetic route to potentially bioactive taxanes much shorter in a medicinal chemistry context.

A total synthesis approach to specifically access Taxol® (**1.1**), whether by convergent routes or by two-phase logic, is unlikely to be competitive with the current, fully enzymatic approach (PCF). However, the lessons learned in taxane chemistry in the event of a renewed interest in taxane-based drug design, the perspective gained surrounding the utility of the two-phase logic in total synthesis, and the new methods developed,[49,68,101,103,164–166,167,168] are worthy returns for a 13-year synthetic campaign to Taxol® (**1.1**).

AUTHOR INFORMATION

Corresponding Author

*E-mail: pbaran@scripps.edu

Present Address

† Vertex Pharmaceuticals, 3215 Merryfield Row, San Diego, California 92121, United States.

Biographies

Yuzuru Kanda completed his undergraduate education at University of Tokyo in 2015 while doing research in Prof. Eiichi Nakamura's lab. Afterwards, he moved to Scripps Research to complete his Ph.D. under the supervision of Prof. Phil S. Baran. He is currently a postdoctoral fellow in Prof. Alexander Radosevich's lab at Massachusetts Institute of Technology.

Yoshihiro Ishihara was born in Japan but was raised in Canada. He received a B.Sc. and M.Sc. in Chemistry at McGill University, and a Ph.D. in 2012 with Prof. Phil S. Baran at Scripps Research. He is currently a medicinal chemist at Vertex Pharmaceuticals (San Diego, CA).

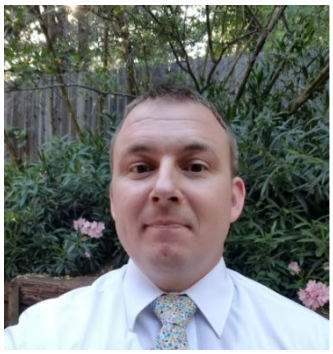

Nathan C. Wilde completed his undergraduate education at Brigham Young University in 2011. After earning his Ph.D. at Scripps Research under Prof. Phil S. Baran in 2015, he pursued postdoctoral studies at Harvard University with E. J. Corey until 2017, at which point he started a career in process chemistry at Vertex Pharmaceuticals (San Diego, CA).

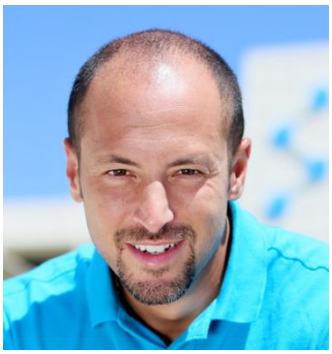

Phil S. Baran completed his undergraduate education at New York University in 1997. After earning his Ph.D. at Scripps Research in 2001, he pursued postdoctoral studies at Harvard University until 2003, at which point he returned to Scripps Research to begin his independent career. He was promoted to the rank of professor in 2008 and is currently the Darlene Shiley Professor of Chemistry. The mission of his laboratory is to educate students at the intersection of fundamental organic chemistry and translational science.

ACKNOWLEDGMENT

This perspective is dedicated with admiration and respect to the late Prof. Robert M. Williams, a great contributor to the taxane field, for his kind encouragement and sage advice. We are grateful to the many Baran lab members that tirelessly contributed to this work, including: Drs. Ke Chen, Abraham Mendoza, Minetaka Isomura, Changxia Yuan, Yehua Jin, Shigenobu Umemiya, and Hugh Nakamura. Our brilliant collaborators at Chemveda Drs. Ravi Kumar Puthukanoori, Venkata Ramana Murthy Appala, Gopi Krishna Gaddamanugu, and Bheema Rao Paraselli truly made the final push towards **1.1** possible. In addition, P.S.B thanks early laboratory members for their critical, high-energy discussions and advice in 2005-2006 that led to the beginning of this project (Drs. Noah Z. Burns, Thomas J. Maimone, Ryan A. Shenvi, and Carlos A. Guerrero). Financial support for this work was provided by NIH (GM-118176), Funai overseas scholarship (predoctoral fellowship to Y. K.), Honjo international scholarship (predoctoral fellowship to Y. K.). The early stages of this program were funded in part by grants from TEVA, LEO Pharma, Bristol-Myers Squibb, and Scripps Research. We thank D.-H. Huang and L. Pasternack (Scripps Research) for assistance with NMR spectroscopy; M. Gembicky (University of California, San Diego) for assistance with X-ray crystallography; Dr. J. S. Chen, B. B. Sanchez and E. Sturgell (Scripps Research) for assistance with LCMS analysis and HRMS analysis. We thank Dr. Julien Vantourout (Scripps Research) for insightful discussions and proofreading of this manuscript. Finally, we are very grateful to Dr. Brendan Burkett for his amazing artwork that was used for the cover piece.

REFERENCES

(1) Nicolaou, K. C.; Montagnon, T. *Molecules That Changed the World: A Brief History of the Art and Science of Synthesis and Its Impact on Society*, 1st ed.; Wiley-VCH:

Weinheim, 2008.
(2) Suffness, M. *TAXOL: Science and Applications*; CRC Press: Boca Raton, 1995.
(3) Brickley, P. NIH Censured for Taxol Deal. *Genome Biol.* **2003**, *4*.
(4) Drugs@FDA: FDA-Approved Drugs: Taxol (Paclitaxel) #020262 https://www.accessdata.fda.gov/scripts/cder/daf/index.cfm?event=overview.process&ApplNo=020262 (accessed Feb 12, 2020).
(5) Celgene. Press Release Archive https://ir.celgene.com/press-releases-archive/default.aspx (accessed May 27, 2020).
(6) Drug Approval Package: Taxotere (Docetaxel) #020449s028 https://www.accessdata.fda.gov/drugsatfda_docs/nda/2004/20-449s028_Taxotere.cfm (accessed Feb 11, 2020).
(7) WHO. Model Lists of Essential Medicines https://www.who.int/medicines/publications/essentialmedicines/en/ (accessed May 27, 2020).
(8) Holton, R. A. Method for Preparation of Taxol. EP0400971 (A2), 1990.
(9) Ojima, I.; Habus, I.; Zhao, M.; Zucco, M.; Park, Y. H.; Sun, C. M.; Brigaud, T. New and Efficient Approaches to the Semisynthesis of Taxol and Its C-13 Side Chain Analogs by Means of β-Lactam Synthon Method. *Tetrahedron* **1992**, *48*, 6985–7012.
(10) Denis, J. N.; Greene, A. E.; Guénard, D.; Guéritte-Voegelein, F.; Mangatal, L.; Potier, P. A Highly Efficient, Practical Approach to Natural Taxol. *J. Am. Chem. Soc.* **1988**, *110*, 5917–5919.
(11) Cino, P. M.; Schwarz, S. R.; Cazzulino, D. L. Callus Cell Induction from Partially Submerged Explant Tissue in Liquid Medium for Preparation of Taxanes. US5527702A, 1996.
(12) Bringi, V.; Kadkade, P. G.; Prince, C. L.; Roach, B. L. Enhanced Production of Taxol and Taxanes by Cell Cultures of Taxus Species. US7264951B1, 2007.
(13) Wang, Y. F.; Shi, Q. W.; Dong, M.; Kiyota, H.; Gu, Y. C.; Cong, B. Natural Taxanes: Developments since 1828. *Chem. Rev.* **2011**, *111*, 7652–7709.
(14) Nicolaou, K. C.; Sorensen, E. J. *Classics in Total Synthesis*, 6th ed.; Wiley-VCG: Weinheim, 2014.
(15) Hudlicky, T.; Reed, W. J. *The Way of Synthesis: Evolution of Design and Methods for Natural Products*, 1st ed.; Wiley-VCH: Weinheim, 2007.
(16) Wender, P. A.; Mucciaro, T. P. A New and Practical Approach to the Synthesis of Taxol and Taxol Analogues: The Pinene Path. *J. Am. Chem. Soc.* **1992**, *114*, 5878–5879.
(17) Holton, R. A.; Somoza, C.; Kim, H.; Liang, F.; Biediger, R. J.; Boatman, P. D.; Shindo, M.; Smith, C. C.; Kim, S.; Nadizadeh, H.; Suzuki, Y.; Tao, C.; Vu, P.; Tang, S.; Zhang, P.; Murthi, K. K.; Gentile, L. N.; Liu, J. H. First Total Synthesis of Taxol. 1. Functionalisation of B Ring. *J. Am. Chem. Soc* **1994**, *116*, 1597–1598.
(18) Holton, R. A.; Kim, H. B.; Somoza, C.; Liang, F.; Biediger, R. J.; Boatman, P. D.; Shindo, M.; Smith, C. C.; Kim, S.; Nadizadeh, H.; Suzuki, Y.; Tao, C.; Vu, P.; Tang, S.; Zhang, P.; Murthi, K. K.; Gentile, L. N.; Liu, J. H. First Total Synthesis of Taxol. 2. Completion of the C and D Rings. *J. Am. Chem. Soc.* **1994**, *116*, 1599–1600.
(19) Nicolaou, K. C.; Yang, Z.; Liu, J. J.; Ueno, H.; Nantermet, P. G.; Guy, R. K.; Claiborne, C. F.; Renaud, J.; Couladouros, E. A.; Paulvannan, K.; Sorensen, E. J. Total Synthesis of Taxol. *Nature* **1994**, *367*, 630–634.
(20) Masters, J. J.; Link, J. T.; Snyder, L. B.; Young, W. B.; Danishefsky, S. J. A Total Synthesis of Taxol. *Angew. Chem. Int. Ed.* **1995**, *34*, 1723–1726.
(21) Wender, P. A.; Badham, N. F.; Conway, S. P.; Floreancig, P. E.; Glass, T. E.; Granicher, C.; Houze, J. B.; Janichen, J.; Lee, D.; Marquess, D. G.; McGrane, P. L.; Meng, W.; Mucciaro, T. P.; Muhlebach, M.; Natchus, M. G.; Paulsen, H.; Rawlins, D. B.; Satkofsky, J.; Shuker, A. J.; Sutton, J. C.; Taylor, R. E.; Tomooka, K. The Pinene Path to Taxanes. 5. Stereocontrolled Synthesis of a Versatile Taxane Precursor. *J. Am. Chem. Soc.* **1997**, *119*, 2755–2756.
(22) Wender, P. A.; Badham, N. F.; Conway, S. P.; Floreancig, P. E.; Glass, T. E.; Houze, J. B.; Krauss, N. E.; Lee, D.; Marquess, D. G.; McGrane, P. L.; Meng, W.; Natchus, M. G.; Shuker, A. J.; Sutton, J. C.; Taylor, R. E. The Pinene Path to Taxanes. 6. A Concise Stereocontrolled Synthesis of Taxol. *J. Am. Chem. Soc.* **1997**, *119*, 2757–2758.
(23) Morihira, K.; Hara, R.; Kawahara, S.; Nishimori, T.; Nakamura, N.; Kusama, H.; Kuwajima, I. Enantioselective Total Synthesis of Taxol. *J. Am. Chem. Soc.* **1998**, *120*, 12980–12981.
(24) Mukaiyama, T.; Shiina, I.; Iwadare, H.; Sakoh, H.; Tani, Y.; Hasegawa, M.; Satoh, K. Asymmetric Total Synthesis of Taxol. *Chem. Eur. J.* **1998**, *5*, 121–161.
(25) Lim, J. A Total Synthesis of Taxol, Harvard University, 2000.
(26) Doi, T.; Fuse, S.; Miyamoto, S.; Nakai, K.; Sasuga, D.; Takahashi, T. A Formal Total Synthesis of Taxol Aided by an Automated Synthesizer. *Chem. Asian J.* **2006**, *1*, 370–383.
(27) Hirai, S.; Utsugi, M.; Iwamoto, M.; Nakada, M. Formal Total Synthesis of (–)-Taxol through Pd-Catalyzed Eight-Membered Carbocyclic Ring Formation. *Chem. Eur. J.* **2015**, *21*, 355–359.
(28) Fukaya, K.; Tanaka, Y.; Sato, A. C.; Kodama, K.; Yamazaki, H.; Ishimoto, T.; Nozaki, Y.; Iwaki, Y. M.; Yuki, Y.; Umei, K.; Sugai, T.; Yamaguchi, Y.; Watanabe, A.; Oishi, T.; Sato, T.; Chida, N. Synthesis of Paclitaxel. 1. Synthesis of the ABC Ring of Paclitaxel by SmI2-Mediated Cyclization. *Org. Lett.* **2015**, *17*, 2570–2573.
(29) Fukaya, K.; Kodama, K.; Tanaka, Y.; Yamazaki, H.; Sugai, T.; Yamaguchi, Y.; Watanabe, A.; Oishi, T.; Sato, T.; Chida, N. Synthesis of Paclitaxel. 2. Construction of the ABCD Ring and Formal Synthesis. *Org. Lett.* **2015**, *17*, 2574–2577.
(30) Imamura, Y.; Yoshioka, S.; Nagatomo, M.; Inoue, M. Total Synthesis of 1-Hydroxytaxinine. *Angew. Chem. Int. Ed.* **2019**, *58*, 12159–12163.
(31) Scherübl, M. Studies Toward the Total Synthesis of Paclitaxel, University of California, Berkeley, 2017.
(32) Corey, E. J.; Cheng, X.-M. *The Logic of Chemical Synthesis*, 1st ed.; John Wiley & Sons Ltd: New York, 1995.
(33) Chen, K.; Baran, P. S. Total Synthesis of Eudesmane Terpenes by Site-Selective C-H Oxidations. *Nature* **2009**, *459*, 824–828.
(34) Chen, K.; Ishihara, Y.; Galán, M. M.; Baran, P. S. Total Synthesis of Eudesmane Terpenes: Cyclase Phase. *Tetrahedron* **2010**, *66*, 4738–4744.
(35) Jørgensen, L.; McKerrall, S. J.; Kuttruff, C. A.; Ungeheuer, F.; Felding, J.; Baran, P. S. 14-Step Synthesis of (+)-Ingenol from (+)-3-Carene. *Science* **2013**, *341*, 878–882.
(36) Jin, Y.; Yeh, C. H.; Kuttruff, C. A.; Jørgensen, L.; Dünstl, G.; Felding, J.; Natarajan, S. R.; Baran, P. S. C-H Oxidation of Ingenanes Enables Potent and Selective Protein Kinase C Isoform Activation. *Angew. Chem. Int. Ed.* **2015**, *54*, 14044–14048.
(37) McKerrall, S. J.; Jørgensen, L.; Kuttruff, C. A.; Ungeheuer, F.; Baran, P. S. Development of a Concise Synthesis of (+)-Ingenol. *J. Am. Chem. Soc.* **2014**, *136*, 5799–5810.
(38) Kawamura, S.; Chu, H.; Felding, J.; Baran, P. S. Nineteen-Step Total Synthesis of (+)-Phorbol. *Nature* **2016**, *532*, 90–93.
(39) Chu, H.; Smith, J. M.; Felding, J.; Baran, P. S. Scalable Synthesis of (-)-Thapsigargin. *ACS Cent. Sci.* **2017**, *3*, 47–51.
(40) Chu, H.; Dünstl, G.; Felding, J.; Baran, P. S. Divergent Synthesis of Thapsigargin Analogs. *Bioorg. Med. Chem. Lett.* **2018**, *28*, 2705–2707.
(41) Kuroda, Y.; Nicacio, K. J.; da Silva-Jr, I. A.; Leger, P. R.; Chang, S.; Gubiani, J. R.; Deflon, V. M.; Nagashima, N.; Rode, A.; Blackford, K.; Ferreira, A. G.; Sette, L. D.; Williams, D. E.; Andersen, R. J.; Jancar, S.; Berlinck, R. G. S.; Sarpong, R. Isolation, Synthesis and Bioactivity Studies of Phomactin Terpenoids. *Nat. Chem.* **2018**, *10*, 938–945.

(42) Condakes, M. L.; Hung, K.; Harwood, S. J.; Maimone, T. J. Total Syntheses of (-)-Majucin and (-)-Jiadifenoxolane A, Complex Majucin-Type Illicium Sesquiterpenes. *J. Am. Chem. Soc.* **2017**, *139*, 17783–17786.

(43) Hung, K.; Condakes, M. L.; Novaes, L. F. T.; Harwood, S. J.; Morikawa, T.; Yang, Z.; Maimone, T. J. Development of a Terpene Feedstock-Based Oxidative Synthetic Approach to the Illicium Sesquiterpenes. *J. Am. Chem. Soc.* **2019**, *141*, 3083–3099.

(44) Wein, L. A.; Wurst, K.; Angyal, P.; Weisheit, L.; Magauer, T. Synthesis of (-)-Mitrephorone A via a Bioinspired Late Stage C-H Oxidation of (-)-Mitrephorone B. *J. Am. Chem. Soc.* **2020**, *141*, 19589–19593.

(45) Berger, M.; Knittl-Frank, C.; Bauer, S.; Winter, G.; Maulide, N. Application of Relay C–H Oxidation Logic to Polyhydroxylated Oleanane Triterpenoids. *Chem* **2020**, *6*, 1183–1189.

(46) Renata, H.; Zhou, Q.; Baran, P. S. Strategic Redox Relay Enables A Scalable Synthesis of Ouabagenin, A Bioactive Cardenolide. *Science* **2013**, *339*, 59–63.

(47) Renata, H.; Zhou, Q.; Dünstl, G.; Felding, J.; Merchant, R. R.; Yeh, C. H.; Baran, P. S. Development of a Concise Synthesis of Ouabagenin and Hydroxylated Corticosteroid Analogues. *J. Am. Chem. Soc.* **2015**, *137*, 1330–1340.

(48) Michaudel, Q.; Journot, G.; Regueiro-Ren, A.; Goswami, A.; Guo, Z.; Tully, T. P.; Zou, L.; Ramabhadran, R. O.; Houk, K. N.; Baran, P. S. Improving Physical Properties via C-H Oxidation: Chemical and Enzymatic Approaches. *Angew. Chem. Int. Ed.* **2014**, *53*, 12091–12096.

(49) See, Y. Y.; Herrmann, A. T.; Aihara, Y.; Baran, P. S. Scalable C-H Oxidation with Copper: Synthesis of Polyoxypregnanes. *J. Am. Chem. Soc.* **2015**, *137*, 13776–13779.

(50) Baran, P. S. Induction Ceremony 2015: Presentations by New Members. *Bull. Am. Acad. Arts Sci.* 63–64.

(51) Mendoza, A.; Ishihara, Y.; Baran, P. S. Scalable Enantioselective Total Synthesis of Taxanes. *Nat. Chem.* **2012**, *4*, 21–25.

(52) Ishihara, Y.; Mendoza, A.; Baran, P. S. Total Synthesis of Taxane Terpenes: Cyclase Phase. *Tetrahedron* **2013**, *69*, 5685–5701.

(53) Ajikumar, P. K.; Xiao, W. H.; Tyo, K. E. J.; Wang, Y.; Simeon, F.; Leonard, E.; Mucha, O.; Phon, T. H.; Pfeifer, B.; Stephanopoulos, G. Isoprenoid Pathway Optimization for Taxol Precursor Overproduction in Escherichia Coli. *Science* **2010**, *330*, 70–74.

(54) Ishihara, Y.; Baran, P. S. Two-Phase Terpene Total Synthesis: Historical Perspective and Application to the Taxol® Problem. *Synlett* **2010**, *12*, 1733–1745.

(55) MacEachern-Keith, G. J.; Wagner Butterfield, L. J.; Incorvia Mattina, M. J. Paclitaxel Stability in Solution. *Anal. Chem.* **1997**, *69*, 72–77.

(56) Wittman, M. D.; Altstadt, T. J.; Kadow, J. F.; Kingston, D. G. I.; Liang, X. 7-Deoxy-6-Substituted Paclitaxels. US5773461A, 1997.

(57) Chen, S.; Wei, J.; Vyas, D. M.; Doyle, T. W.; Farina, V. A Facile Synthesis of 7,10-Dideoxy Taxol and 7-Epi-10-Deoxy Taxol. *Tetrahedron Lett.* **1993**, *34*, 6845–6848.

(58) Klein, L. L.; Maring, C. J.; Li, L.; Yeung, C. M.; Thomas, S. A.; Grampovnik, D. J.; Plattner, J. J.; Henry, R. F. Synthesis of Ring B-Rearranged Taxane Analogs. *J. Org. Chem.* **1994**, *59*, 2370–2373.

(59) Samaranayake, G.; Magri, N. F.; Jitrangsri, C.; Kingston, D. G. I. Modified Taxols. 5.1 Reaction of Taxol with Electrophilic Reagents and Preparation of Rearranged Taxol Derivative with Tubulin Assembly Activity. *J. Org. Chem.* **1991**, *56*, 5114–5119.

(60) Lee, D.; Kim, M. J. Enzymatic Selective Dehydration and Skeleton Rearrangement of Paclitaxel Precursors. *Org. Lett.* **1999**, *1*, 925–927.

(61) Croteau, R.; Ketchum, R. E. B.; Long, R. M.; Kaspera, R.; Wildung, M. R. Taxol Biosynthesis and Molecular Genetics. *Phytochem. Rev.* **2006**, *5*, 75–97.

(62) Jennewein, S.; Wildung, M. R.; Chau, M. D.; Walker, K.; Croteau, R. Random Sequencing of an Induced Taxus Cell CDNA Library for Identification of Clones Involved in Taxol Biosynthesis. *Proc. Natl. Acad. Sci. U. S. A.* **2004**, *101*, 9149–9154.

(63) Davis, E. M.; Croteau, R. Cyclization Enzymes in the Biosynthesis of Monoterpenes, Sesquiterpenes, and Diterpenes. In *Biosynthesis Aromatic Polyketides, Isoprenoids, Alkaloids*; Springer: New York, 2000; pp 53–96.

(64) Ishihara, Y. A Two-Phase Approach to Terpene Total Synthesis : Demonstration of a " Cyclase-Phase " Synthesis of the Eudesmane and Taxane Families, The Scripps Research Institute, 2012.

(65) Wilde, N. C. The Two-Phase Synthesis of Taxane Natural Products : Developing the Tools for the Oxidase Phase, The Scripps Research Institute, 2016.

(66) Kanda, Y. Two-Phase Synthesis of Taxol®, Scripps Research, 2020.

(67) Kanda, Y.; Nakamura, H.; Umemiya, S.; Puthukanoori, R. K.; Appala, V. R. M.; Gaddamanugu, G. K.; Paraselli, B. R.; Baran, P. Two-Phase Synthesis of Taxol®. *J. Am. Chem. Soc.* **2020**, *142*, 10526–10533.

(68) Wilde, N. C.; Isomura, M.; Mendoza, A.; Baran, P. S. Two-Phase Synthesis of (–)-Taxuyunnanine D. *J. Am. Chem. Soc.* **2014**, *136*, 4909–4912.

(69) Yuan, C.; Jin, Y.; Wilde, N. C.; Baran, P. S. Short, Enantioselective Total Synthesis of Highly Oxidized Taxanes. *Angew. Chem. Int. Ed.* **2016**, *55*, 8280–8284.

(70) Holton, R. A.; Juo, R. R.; Kim, H. B.; Williams, A. D.; Harusawa, S.; Lowenthal, R. E.; Yogai, S. A Synthesis of Taxusin. *J. Am. Chem. Soc.* **1988**, *110*, 6558–6560.

(71) Hara, R.; Furukawa, T.; Horiguchi, Y.; Kuwajima, I. Total Synthesis of (±)-Taxusin. *J. Am. Chem. Soc.* **1996**, *118*, 9186–9187.

(72) Hara, R.; Furukawa, T.; Kashima, H.; Kusama, H.; Horiguchi, Y.; Kuwajima, I. Enantioselective Total Synthesis of (+)-Taxusin. *J. Am. Chem. Soc.* **1999**, *121*, 3072–3082.

(73) Paquette, L. A.; Zhao, M. Enantiospecific Total Synthesis of Natural (+)-Taxusin. 1. Retrosynthesis, Advancement to Diastereomeric Trans-Δ9,10-Tricyclic Olefinic Intermediates, and the Stereocontrol Attainable Because of Intrinsic Rotational Barriers Therein. *J. Am. Chem. Soc.* **1998**, *120*, 5203–5212.

(74) Paquette, L. A.; Wang, H. L.; Su, Z.; Zhao, M. Enantiospecific Total Synthesis of Natural (+)-Taxusin. 2. Functionalization of the A-Ring and Arrival at the Target. *J. Am. Chem. Soc.* **1998**, *120*, 5213–5225.

(75) Zhang, H.; Takeda, Y.; Minami, Y.; Yoshida, K.; Matsumoto, T.; Xiang, W.; Mu, O.; Sun, H. Three New Taxanes from the Roots of Taxus Yunnanensis. *Chem. Lett.* **1994**, *23*, 957–960.

(76) Izawa, Y.; Pun, D.; Stahl, S. S. Palladium-Catalyzed Aerobic Dehydrogenation of Substituted Cyclohexanones to Phenols. *Science* **2011**, *33*, 209–214.

(77) Heumann, A.; Åkermark, B. Oxidation with Palladium Salts: Catalytic Preparation of Allyl Acetates from Monoolefins Using a Three-Component Oxidation System. *Angew. Chem. Int. Ed.* **1984**, *23*, 453–454.

(78) Hansson, S.; Rein, T.; Åkermark, B.; Heumann, A. Preparation of Allylic Acetates from Simple Alkenes by Palladium(II)-Catalyzed Acetoxylation. *J. Org. Chem.* **1990**, *55*, 975–984.

(79) Bäckvall, J. E.; Hopkins, B. R.; Grennberg, H.; Mader, M. M.; Awasthi, A. K. Multistep Electron Transfer in Palladium-Catalyzed Aerobic Oxidations via a Metal Macrocycle-Quinone System. *J. Am. Chem. Soc.* **1990**, *112*, 5160–5166.

(80) Kende, A. S.; Johnson, S.; Sanfilippo, P.; Hodges, J. C.; Junheim, L. N. Synthesis of a Taxane Triene. *J. Am. Chem. Soc.* **1986**, *108*, 3513–3515.

(81) Salmond, W. G.; Barta, M. A.; Havens, J. L. Allylic Oxidation with 3,5-Dimethylpyrazole. Chromium Trioxide

Complex. Steroidal Δ5-7-Ketones. *J. Org. Chem.* **1978**, *43*, 2057–2059.
(82) Collins, J. C.; Hess, W. W.; Frank, F. J. Dipyridine-Chromium(VI) Oxide Oxidation of Alcohols in Dichloromethane. *Tetrahedron Lett.* **1968**, *9*, 3363–3366.
(83) Samsel, E. G.; Srinivasan, K.; Kochi, J. K. Mechanism of the Chromium-Catalyzed Epoxidation of Olefins. Role of Oxochromium(V) Cations. *J. Am. Chem. Soc.* **1985**, *107*, 7606–7617.
(84) Krumpolc, M.; Roček, J. Chromium(V) Oxidations of Organic Compounds. *Inorg. Chem.* **1985**, *24*, 617–621.
(85) Babler, J. H.; Coghlan, M. J. A Facile Method For The Bishomologation Of Ketones To α,β-Unsaturated Aldehydes: Application To The Synthesis Of The Cyclohexanoid Components Of The Boll Weevil Sex Attractant. *Synth. Commun.* **1976**, *6*, 469–474.
(86) Dauben, W. G.; Michno, D. M. Direct Oxidation of Tertiary Allylic Alcohols. A Simple and Effective Method for Alkylative Carbonyl Transposition. *J. Org. Chem.* **1977**, *42*, 682–685.
(87) Loskot, S. A.; Romney, D. K.; Arnold, F. H.; Stoltz, B. M. Enantioselective Total Synthesis of Nigelladine A via Late-Stage C-H Oxidation Enabled by an Engineered P450 Enzyme. *J. Am. Chem. Soc.* **2017**, *139*, 10196–10199.
(88) Schuppe, A. W.; Huang, D.; Chen, Y.; Newhouse, T. R. Total Synthesis of (-)-Xylogranatopyridine B via a Palladium-Catalyzed Oxidative Stannylation of Enones. *J. Am. Chem. Soc.* **2018**, *140*, 2062–2066.
(89) Wu, Y.; Huang, J. H.; Shen, X.; Hu, Q.; Tang, C. J.; Li, L. Facile Cleavage of Triethylsilyl (TES) Ethers Using o-Lodoxybenzoic Acid (IBX) without Affecting Tert-Butyldimethylsilyl (TBS) Ethers. *Org. Lett.* **2002**, *4*, 2141–2144.
(90) De Marcano, D. P. D. C.; Halsall, T. G. The Isolation of Seven New Taxane Derivatives from the Heartwood of Yew (Taxus Baccata L.). *J. Chem. Soc. D Chem. Commun.* **1969**, *4*, 1282–1283.
(91) Bouveault, L.; Blanc, G. L. Préparation Des Alcools Primaires Au Moyen Des Acides Correspondants. *Bull. Soc. Chim. Fr.* **1903**, *136*, 1676–1678.
(92) Chong, A. O.; Sharpless, K. B. On the Mechanism of the Molybdenum and Vanadium Catalyzed Epoxidation of Olefins by Alkyl Hydroperoxides. *J. Org. Chem.* **1977**, *42*, 1587–1590.
(93) Vedejs, E. A Method for Direct Hydroxylation of Enolates. Transition Metal Peroxide Reactions. *J. Am. Chem. Soc.* **1974**, *96*, 5944–5946.
(94) Pulicani, J. P.; Bourzat, J. D.; Bouchard, H.; Commerçon, A. Electrochemical Reduction of Taxoids: Selective Preparation of 9-Dihydro-, 10-Deoxy- and 10-Deacetoxy-Taxoids. *Tetrahedron Lett.* **1994**, *35*, 4999–5002.
(95) Tahara, K.; Shimakoshi, H.; Tanaka, A.; Hisaeda, Y. Synthesis and Characterization of Vitamin B12-Hyperbranched Polymer. *Tetrahedron Lett.* **2007**, *48*, 5065–5068.
(96) Chen, Y. J.; Chen, C. Y.; Shen, Y. C. New Taxoids from the Seeds of Taxus Chinensis. *J. Nat. Prod.* **1999**, *62*, 149–151.
(97) Schönecker, B.; Zheldakova, T.; Liu, Y.; Kötteritzsch, M.; Günther, W.; Görls, H. Biomimetic Hydroxylation of Nonactivated CH2 Groups with Copper Complexes and Molecular Oxygen. *Angew. Chem. Int. Ed.* **2003**, *42*, 3240–3244.
(98) Baldwin, J. E.; Nájera, C.; Yus, M. Oxidation of Unactivated Methyl Groups via a Cyclopalladation Reaction. *J. Chem. Soc. Chem. Commun.* **1985**, 126–127.
(99) Neber, P. W.; Hartung, K.; Ruopp, W. Die Stereoisomeren Formen Des O-Nitrobenzyl-methyl-ketoxims. *Chem. Ber.* **1925**, *58*, 1234–1246.
(100) Ni, J.; Ozawa, J.; Oisaki, K.; Kanai, M. Directing Activator-Assisted Regio- and Oxidation State-Selective Aerobic Oxidation of Secondary C(Sp3)-H Bonds in Aliphatic Alcohols. *Org. Biomol. Chem.* **2016**, *14*, 4378–4381.
(101) Voica, A. F.; Mendoza, A.; Gutekunst, W. R.; Fraga, J. O.; Baran, P. S. Guided Desaturation of Unactivated Aliphatics. *Nat. Chem.* **2012**, *4*, 629–635.
(102) Parasram, M.; Chuentragool, P.; Sarkar, D.; Gevorgyan, V. Photoinduced Formation of Hybrid Aryl Pd-Radical Species Capable of 1,5-HAT: Selective Catalytic Oxidation of Silyl Ethers into Silyl Enol Ethers. *J. Am. Chem. Soc.* **2016**, *138*, 6340–6343.
(103) Chen, K.; Richter, J. M.; Baran, P. S. 1,3-Diol Synthesis via Controlled, Radical-Mediated C-H Functionalization. *J. Am. Chem. Soc.* **2008**, *130*, 7247–7249.
(104) Stork, G.; Kahn, M. Control of Ring Junction Stereochemistry via Radical Cyclization. *J. Am. Chem. Soc.* **1985**, *107*, 500–501.
(105) Kasuya, S.; Kamijo, S.; Inoue, M. Direct Construction of 1,3-Diaxial Diol Derivatives by C-H Hydroxylation. *Org. Lett.* **2009**, *11*, 3630–3632.
(106) Wong, M. K.; Chung, N. W.; He, L.; Wang, X. C.; Yan, Z.; Tang, Y. C.; Yang, D. Investigation on the Regioselectivities of Intramolecular Oxidation of Unactivated C-H Bonds by Dioxiranes Generated in Situ. *J. Org. Chem.* **2003**, *68*, 6321–6328.
(107) Li, B.; Driess, M.; Hartwig, J. F. Iridium-Catalyzed Regioselective Silylation of Secondary Alkyl C-H Bonds for the Synthesis of 1,3-Diols. *J. Am. Chem. Soc.* **2014**, *136*, 6586–6589.
(108) Breslow, R.; Gellman, S. H. Intramolecular Nitrene C-H Insertions Mediated by Transition-Metal Complexes as Nitrogen Analogues of Cytochrome P-450 Reactions. *J. Am. Chem. Soc.* **1983**, *105*, 6728–6729.
(109) Espino, C. G.; Wehn, P. M.; Chow, J.; Du Bois, J. Synthesis of 1,3-Difunctionalized Amine Derivatives through Selective C-H Bond Oxidation. *J. Am. Chem. Soc.* **2001**, *123*, 6935–6936.
(110) Asensio, G.; Castellano, G.; Mello, R.; González Núñez, M. E. Oxyfunctionalization of Aliphatic Esters by Methyl(Trifluoromethyl)Dioxirane. *J. Org. Chem.* **1996**, *61*, 5564–5566.
(111) Bigi, M. A.; Reed, S. A.; White, M. C. Diverting Non-Haem Iron Catalysed Aliphatic C-H Hydroxylations towards Desaturations. *Nat. Chem.* **2011**, *3*, 216–222.
(112) Barton, D. H. R.; Bringmann, G.; Lamotte, G.; Motherwell, W. B.; Motherwell, R. S. H.; Porter, A. E. A. Reactions of Relevance to the Chemistry of Aminoglycoside Antibiotics. Part 14. A Useful Radical-Deamination Reaction. *J. Chem. Soc. Perkin Trans. 1* **1980**, 2657–2664.
(113) Hartwig, J. F. Evolution of C-H Bond Functionalization from Methane to Methodology. *J. Am. Chem. Soc.* **2016**, *138*, 2–24.
(114) Horiguchi, T.; Nagura, M.; Cheng, Q.; Oritani, T.; Kudo, T. Chemical Oxidation of Taxoids with M-CPBA and Dimethyl Dioxirane: Regioselective Epoxidation of Taxinine J Derivatives. *Heterocycles* **2000**, *53*, 2629–2642.
(115) Maier, W. F.; von Ragué Schleyer, P. Evaluation and Prediction of the Stability of Bridgehead Olefins. *J. Am. Chem. Soc.* **1981**, *103*, 1891–1900.
(116) McEwen, A. B.; von Ragué Schleyer, P. Hyperstable Olefins: Further Calculational Explorations and Predictions. *J. Am. Chem. Soc.* **1986**, *108*, 3951–3960.
(117) Murray, R. W.; Gu, H. Dimethyldioxirane Reactions: Rate Acceleration Due to Intramolecular H-Bonding. *J. Phys. Org. Chem.* **1996**, *9*, 751–758.
(118) Angelis, Y. S.; Hatzakis, N. S.; Smonou, I.; Orfanopoulos, M. Oxidation of Benzyl Alcohols by Dimethyldioxirane. The Question of Concerted versus Stepwise Mechanisms Probed by Kinetic Isotope Effects. *Tetrahedron Lett.* **2001**, *42*, 3753–3756.
(119) Yang, Z.; Yu, P.; Houk, K. N. Molecular Dynamics of Dimethyldioxirane C-H Oxidation. *J. Am. Chem. Soc.* **2016**, *138*, 4237–4242.
(120) Clive, D. L. J.; Cantin, M.; Khodabocus, A.; Kong, X.; Tao, Y. Protecting Group Improvement by Isotopic Substitution: Synthesis of the Quinone System of Fredericamycin A. *Tetrahedron* **1993**, *49*, 7917–7930.
(121) Vedejs, E.; Little, J. Aziridinomitosenes by Anionic

Cyclization: Deuterium as a Removable Blocking Group. *J. Am. Chem. Soc.* **2002**, *124*, 748–749.
(122) Miyashita, M.; Sasaki, M.; Hattori, I.; Sakai, M.; Tanino, K. Total Synthesis of Norzoanthamine. *Science* **2004**, *305*, 495–499.
(123) Quasdorf, K. W.; Huters, A. D.; Lodewyk, M. W.; Tantillo, D. J.; Garg, N. K. Total Synthesis of Oxidized Welwitindolinones and (-)- N -Methylwelwitindolinone C Isonitrile. *J. Am. Chem. Soc.* **2012**, *134*, 1396–1399.
(124) Anwar, S.; Davis, A. P. The Application of Difunctional Organosilicon Compounds to Organic Synthesis; 1,3-Asymmetric Induction in the Reduction of β-Hydroxy-Ketones. *J. Chem. Soc. Chem. Commun.* **1986**, *11*, 831–832.
(125) Vazquez, A.; Williams, R. M. Studies on the Biosynthesis of Taxol. Synthesis of Taxa-4(20),11(12)-Diene-2α,5α-Diol. *J. Org. Chem.* **2000**, *65*, 7865–7869.
(126) Danishefsky, S. J.; Bornmann, W. G.; Queneau, Y.; Magee, T. V.; Krol, W. J. Total Synthesis of Taxol. WO1993020036A1, 1993.
(127) Takahashi, H.; Mitani, I.; Kusama, H.; Kuwajima, I. Synthetic Studies on Taxinine. In *Tennen Yuki Kagobutsu Toronkai*; Tennen Yuki Kagobutsu Toronkai Koen Yoshishu, 1999.
(128) Szostak, M.; Spain, M.; Procter, D. , SmCl2, and Their Complexes with Water by Reduction of Aromatic Hydrocarbons. Reduction of Anthracene and Stilbene by Samarium (II) Iodide–Water Complex. *J. Org. Chem.* **2014**, *79*, 2522–2537.
(129) Turlik, A.; Chen, Y.; Scruse, A. C.; Newhouse, T. R. Convergent Total Synthesis of Principinol D, a Rearranged Kaurane Diterpenoid. *J. Am. Chem. Soc.* **2019**, *141*, 8088–8092.
(130) An, J.; Work, D. N.; Kenyon, C.; Procter, D. J. Evaluating a Sodium Dispersion Reagent for the Bouveault-Blanc Reduction of Esters. *J. Org. Chem.* **2014**, *79*, 6743–6747.
(131) Zimmerman, H. E. A Mechanistic Analysis of the Birch Reduction. *Acc. Chem. Res.* **2012**, *45*, 164–170.
(132) Ohsawa, T.; Hatano, K.; Kayoh, K.; Kotabe, J.; Oishi, T. Dissolving Metal Reduction with Crown Ether -Reductive Demethylation of Mono-, Di- and Trimethoxybenzene Derivatives with Toluene Radical Anion. *Tetrahedron Lett.* **1992**, *33*, 5555–5558.
(133) Kihara, N.; Ollivier, C.; Renaud, P. Efficient Radical Oxygenation of α-Lodocarboxylic Acid Derivatives. *Org. Lett.* **1999**, *1*, 1419–1422.
(134) Tsunoda, T.; Nagaku, M.; Nagino, C.; Kawamura, Y.; Ozaki, F.; Hioki, H.; Itô, S. Carbon-Carbon Bond Formation with New Mitsunobu Reagents. *Tetrahedron Lett.* **1995**, *36*, 2531–2534.
(135) Tsunoda, T.; Yamamoto, H.; Goda, K.; Itô, S. Mitsunobu-Type Alkylation of p-Toluenesulfonamide. A Convenient New Route to Primary and Secondary Amines. *Tetrahedron Lett.* **1996**, *37*, 2457–2458.
(136) Tsunoda, T.; Nagino, C.; Oguri, M.; Itô, S. Mitsunobu-Type Alkylation with Active Methine Compounds. *Tetrahedron Lett.* **1996**, *37*, 2459–2462.
(137) Jacob, J.; Espenson, J. H.; Jensen, J. H.; Gordon, M. S. 1,3-Transposition of Allylic Alcohols Catalyzed by Methyltrioxorhenium. *Organometallics* **1998**, *17*, 1835–1840.
(138) Bellemin-Laponnaz, S.; Gisie, H.; Le Ny, J. P.; Osborn, J. A. Mechanistic Insights into the Very Efficient [ReO3OSiR3]-Catalyzed Isomerization of Allyl Alcohols. *Angew. Chem. Int. Ed.* **1997**, *36*, 976–978.
(139) Kagiya, T.; Sumida, Y.; Tachi, T. An Infrared Spectroscopic Study of Hydrogen Bonding Interaction. Structural Studies of Proton-Donating and -Accepting Powers. *Bull. Chem. Soc. Jpn.* **1970**, *43*, 3716–3722.
(140) Murray, R. W.; Gu, D. Dioxirane Chemistry. Part 23. The Effect of Solvent on the Dimethyldioxirane Epoxidation Reaction. *J. Chem. Soc. Perkin Trans. 2* **1993**, *11*, 2203–2207.
(141) Gibert, M.; Ferrer, M.; Sänchez-Baeza, F.; Messeguer, A. Availability and Reactivity of Concentrated Dimethyldioxirane Solutions in Solvents Other Than Acetone. *Tetrahedron* **1997**, *53*, 8643–8650.
(142) O'Brien, P.; Pilgram, C. D. Synthesis and Enantioselective Rearrangement of Meso-Aziridino Cyclohexene Oxides. *Tetrahedron Lett.* **1999**, *40*, 8427–8430.
(143) Venturello, C.; D'Aloisio, R. Quaternary Ammonium Tetrakis(Diperoxotungsto)Phosphates(3-) as a New Class of Catalysts for Efficient Alkene Epoxidation with Hydrogen Peroxide. *J. Org. Chem.* **1988**, *53*, 1553–1557.
(144) Taber, D. F.; Neubert, T. D.; Rheingold, A. L. Synthesis of (-)-Morphine. *J. Am. Chem. Soc.* **2002**, *124*, 12416–12417.
(145) Liang, X.; Kingston, D. G. I.; Lin, C. M.; Mamel, E. Synthesis and Biological Evaluation of Paclitaxel Analogs Modified in Ring C. *Tetrahedron Lett.* **1995**, *36*, 2901–2904.
(146) Nugent, W. A.; RajanBabu, T. V. Transition-Metal-Centered Radicals in Organic Synthesis. Titanium(III)-Induced Cyclization of Epoxy Olefins. *J. Am. Chem. Soc.* **1988**, *110*, 8561–8562.
(147) Rosales, A.; Rodríguez-García, I.; Muñoz-Bascõn, J.; Roldan-Molina, E.; Padial, N. M.; Morales, L. P.; García-Ocaña, M.; Oltra, J. E. The Nugent Reagent: A Formidable Tool in Contemporary Radical and Organometallic Chemistry. *European J. Org. Chem.* **2015**, *2015*, 4567–4591.
(148) Gansäuer, A.; Rinker, B. A Comparison of Electron Transfer Reagents in the Reductive Opening of Epoxides: Reasons for the Superiority of Titanocene Based Complexes. *Tetrahedron* **2002**, *58*, 7017–7026.
(149) Morcillo, S. P.; Miguel, D.; Campaña, A. G.; Álvarez De Cienfuegos, L.; Justicia, J.; Cuerva, J. M. Recent Applications of Cp2TiCl in Natural Product Synthesis. *Org. Chem. Front.* **2014**, *1*, 15–33.
(150) Fuji, K.; Watanabe, Y.; Ohtsubo, T.; Nuruzzaman, M.; Hamajima, Y.; Kohno, M. Synthesis of Extremely Simplified Compounds Possessing the Key Pharmacophore Units of Taxol, Phenylisoserine and Oxetane Moieties. *Chem. Pharm. Bull.* **1999**, *47*, 1334–1337.
(151) Fang, W.-S.; Liang, X.-T. Recent Progress in Structure Activity Relationship and Mechanistic Studies of Taxol Analogues. *Mini-Reviews Med. Chem.* **2012**, *5*, 1–12.
(152) Kim, D. E.; Zweig, J. E.; Newhouse, T. R. Total Synthesis of Paspaline A and Emindole PB Enabled by Computational Augmentation of a Transform-Guided Retrosynthetic Strategy. *J. Am. Chem. Soc.* **2019**, *141*, 1479–1483.
(153) Zwick, C.; Sosa, M.; Renata, H. Concise Chemoenzymatic Total Synthesis of GE81112 B1. *ChemRxiv.* **2019**, https://doi.org/10.26434/chemrxiv.9684554.v1.
(154) Newhouse, T.; Baran, P. S. If C-H Bonds Could Talk: Selective C-H Bond Oxidation. *Angew. Chem. Int. Ed.* **2011**, *50*, 3362–3374.
(155) Cernak, T.; Dykstra, K. D.; Tyagarajan, S.; Vachal, P.; Krska, S. W. The Medicinal Chemist's Toolbox for Late Stage Functionalization of Drug-like Molecules. *Chem. Soc. Rev.* **2016**, *45*, 546–576.
(156) Abrams, D. J.; Provencher, P. A.; Sorensen, E. J. Recent Applications of C-H Functionalization in Complex Natural Product Synthesis. *Chem. Soc. Rev.* **2018**, *47*, 8925–8967.
(157) Harvey, A. L.; Edrada-Ebel, R.; Quinn, R. J. The Re-Emergence of Natural Products for Drug Discovery in the Genomics Era. *Nat. Rev. Drug Discov.* **2015**, *14*, 111–129.
(158) Kingston, D. G. I. Taxol: The Chemistry and Structure-Activity Relationships of a Novel Anticancer Agent. *Trends Biotechnol.* **1994**, *12*, 222–227.
(159) He, L.; Jagtap, P. G.; Kingston, D. G. I.; Shen, H. J.; Orr, G. A.; Horwitz, S. B. A Common Pharmacophore for Taxol and the Epothilones Based on the Biological Activity of a Taxane Molecule Lacking a C-13 Side Chain. *Biochemistry* **2000**, *39*, 3972–3978.
(160) Wang, M.; Cornett, B.; Nettles, J.; Liotta, D. C.; Snyder, J. P. The Oxetane Ring in Taxol. *J. Org. Chem.* **2000**, *65*, 1059–1068.
(161) Chaudhary, A. G.; Rimoldi, J. M.; Kingston, D. G. I. Modified Taxols. 10. Preparation of 7-Deoxytaxol, a Highly

Bioactive Taxol Derivative, and Interconversion of Taxol and 7-Epi-Taxol. *J. Org. Chem.* **1993**, *58*, 3798–3799.
(162) Chen, S. H.; Huang, S.; Kant, J.; Fairchild, C.; Wei, J.; Farina, V. Synthesis of 7-Deoxy- and 7,10-Dideoxytaxol via Radical Intermediates. *J. Org. Chem.* **1993**, *58*, 5028–5029.
(163) Kingston, D. G. I. The Shape of Things to Come: Structural and Synthetic Studies of Taxol and Related Compounds. *Phytochemistry* **2007**, *68*, 1844–1854.
(164) Horn, E. J.; Rosen, B. R.; Chen, Y.; Tang, J.; Chen, K.; Eastgate, M. D.; Baran, P. S. Scalable and Sustainable Electrochemical Allylic C-H Oxidation. *Nature* **2016**, *533*, 77–81.
(165) Kawamata, Y.; Yan, M.; Liu, Z.; Bao, D. H.; Chen, J.; Starr, J. T.; Baran, P. S. Scalable, Electrochemical Oxidation of Unactivated C-H Bonds. *J. Am. Chem. Soc.* **2017**, *139*, 7448–7451.
(166) Chen, K.; Eschenmoser, A.; Baran, P. S. Strain Release in C-H Bond Activation? *Angew. Chem. Int. Ed.* **2009**, *48*, 9705–9708.
(167) Michaudel, Q.; Thevenet, D.; Baran, P. S. Intermolecular Ritter-Type C-H Amination of Unactivated Sp 3 Carbons. *J. Am. Chem. Soc.* **2012**, *134*, 2547–2550.
(168) Trammell, R.; See, Y. Y.; Herrmann, A. T.; Xie, N.; Díaz, D. E.; Siegler, M. A.; Baran, P. S.; Garcia-Bosch, I. Decoding the Mechanism of Intramolecular Cu-Directed Hydroxylation of Sp3 C-H Bonds. *J. Org. Chem.* **2017**, *82*, 7887–7904.

GRAPHICAL ABSTRACT